



# MARINE ISOTOPE STAGE 3 SEA LEVEL FLUCTUATIONS: DATA SYNTHESIS AND NEW OUTLOOK

M. Siddall,<sup>1,2</sup> E. J. Rohling,<sup>3</sup> W. G. Thompson,<sup>4</sup> and C. Waelbroeck<sup>5</sup>

Received 2 May 2007; revised 14 April 2008; accepted 16 May 2008; published 5 November 2008.

[1] To develop a better understanding of the abrupt Dansgaard-Oeschger mode of climate change, it is essential that we establish whether the ice sheets are actively involved, as trigger or amplifier, or whether they merely respond in a passive manner. This requires careful assessment of the fundamental issues of magnitude and phasing of global ice volume fluctuations within marine isotope stage 3 (MIS 3), which to date remain enigmatic.

**Citation:** Siddall, M., E. J. Rohling, W. G. Thompson, and C. Waelbroeck (2008), Marine isotope stage 3 sea level fluctuations: Data synthesis and new outlook, *Rev. Geophys.*, 46, RG4003, doi:10.1029/2007RG000226.

## 1. INTRODUCTION: MARINE ISOTOPE STAGE 3 CLIMATIC CONTEXT

[2] Marine isotope stage 3 (MIS 3) is the period between 60 and 25 ka B.P. (B.P. means before present where “present” represents 1950) when climatic conditions fluctuated over a broad range on millennial time scales (Figure 1). The study of MIS 3 may help us to understand how the climate behaves when undergoing rapid changes and therefore might also further increase our understanding of rapid, anthropogenic climate change. To develop a better understanding of these abrupt climate changes during MIS 3, it is essential that we establish whether the ice sheets are actively involved, as trigger or amplifier, or whether they merely respond in a passive manner. This requires careful assessment of the fundamental issues of magnitude and phasing of global ice volume fluctuations within MIS 3, which to date remain enigmatic [e.g., Siddall *et al.*, 2003; Rohling *et al.*, 2004; Knutti *et al.*, 2004; Flückiger *et al.*, 2006; Arz *et al.*, 2007]. Here we review and summarize recent progress on

We review recent advances in observational studies pertaining to these key issues and discuss the implications for modeling studies. Our aim is to construct a robust stratigraphic framework for the MIS 3 period regarding sea level variability, using the most up-to-date arguments available by combining insights from both modeling and observational approaches.

reconstructing eustatic sea level during this period. We consider eustatic sea level variations and not local isostatic effects related to local rebound in areas which might be subject to the “broad-shelf effect” [Bloom, 1967] or glacial rebound. All of the records we show here have either been corrected for these effects or are not affected by them because of their distance from large ice sheets or because isostasy does not affect the records. For example, isostasy does not affect benthic oxygen isotope records. Our aim is to construct a robust stratigraphic framework for the MIS 3 period regarding eustatic sea level variability, using the most up-to-date information available. The various eustatic sea level reconstructions used here are listed in Table 1, and geographic locations are shown in Figure 2.

### 1.1. Broad Context

[3] MIS 3 has been defined by variations in the oxygen isotope record in ocean sediment cores on orbital “Milankovitch” time scales [e.g., Imbrie *et al.*, 1984], where minima in deep-sea benthic stable oxygen isotope records in general correspond to reduced global ice volume and hence to relatively high sea level [e.g., Imbrie *et al.*, 1984; Bassinot *et al.*, 1994; Waelbroeck *et al.*, 2002]. Major peaks and troughs in the oxygen isotope record were assigned a numbered MIS, with odd numbers for interglacials and even numbers for glacials. An exception to this general rule is MIS 3, a period when sea level ranged between 60 and 90 m

<sup>1</sup>Lamont-Doherty Earth Observatory, Palisades, New York, USA.

<sup>2</sup>Now at Department of Earth Sciences, University of Bristol, Bristol, UK.

<sup>3</sup>National Oceanography Centre, Southampton, Southampton, UK.

<sup>4</sup>Woods Hole Oceanographic Institution, Woods Hole, Massachusetts, USA.

<sup>5</sup>Laboratoire des Sciences du Climat et de l'Environnement, IPSL, CEA, CNRS, Gif-sur-Yvette, France.

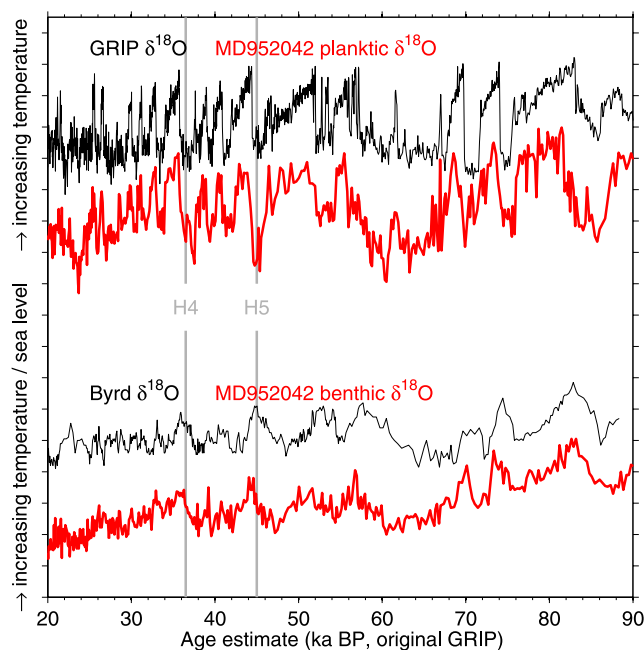


**Figure 1.** The methane synchronized records of the Greenland Ice Core Project (GRIP) (original GRIP time scale) and Byrd after *Blunier et al.* [1998] and *Blunier and Brook* [2001] for comparison with the coregistered planktic and benthic  $\delta^{18}\text{O}$  records of core MD952042 from the Portuguese margin. Vertical gray lines indicate Heinrich events after the review of *Hemming* [2004].

below the present [e.g., *Chappell*, 2002; *Waelbroeck et al.*, 2002; *Siddall et al.*, 2003; this paper] and which therefore cannot be described as an interglacial. Also, MIS 3 occurred between 60 and 25 ka before the present, which would not agree with the “typical”  $\sim 100$ -ka spacing of interglacial periods during the last  $\sim 1$  million years [e.g., *Lisiecki and Raymo*, 2005].

[4] The long-term glacial-interglacial waxing and waning of global ice volume has been broadly linked to summer insolation at  $65^\circ\text{N}$ , the latitude of maximum continentality in the Northern Hemisphere, which corresponds to the position of the large Northern Hemisphere ice sheets [e.g., *Imbrie and Imbrie*, 1979; *Imbrie et al.*, 1984; *Bassinot et al.*, 1994]. This so-called “Milankovitch,” or orbital, insolation forcing of the ice ages [e.g., *Imbrie et al.*, 1984; *Bassinot et al.*, 1994] is dominated by variability in orbital eccentricity (400, 125, and 95 ka), axial tilt (41 ka), and precession (24, 22, and 19 ka). The orbital insolation forcing of the high-latitude northern ice sheets did not fluctuate strongly through MIS 3, but it was higher at the start of MIS 3 than at the end (Figure 3).

## 1.2. Millennial-Scale Variability

[5] Ice core proxy records of high-latitude Northern Hemisphere temperature reveal a distinctive pattern of repeated decadal-scale warming events of  $8^\circ$ – $15^\circ\text{C}$  during MIS 3, known as Dansgaard-Oeschger (D-O) events [e.g., *Blunier et al.*, 1998; *Stuiver and Grootes*, 2000; *Blunier and Brook*, 2001; *Huber et al.*, 2006]. These rapid warmings are

interspersed with cold periods such that MIS 3 is a period of substantial millennial-scale climate variability (Figure 1). This variability is found throughout much of the Northern Hemisphere in marine sediments and also continental records [*Shackleton et al.*, 2000; *Wang et al.*, 2001; *Voelker*, 2002; *Rohling et al.*, 2003; *Denton et al.*, 2005]. *Clark et al.* [2002, 2007] provide a robust evaluation of this pattern of distribution. D-O events often appear clustered in “Bond cycles,” groups of up to four with a longer warm period followed by up to three shorter warm periods, interspersed with cold periods [*Bond and Lotti*, 1995]. These Bond cycles end in a cold period, during which a so-called Heinrich event (i.e., a massive deposition of ice-rafted debris (IRD)) occurs in the North Atlantic between about  $40$  and  $50^\circ\text{N}$  (see overview by *Hemming* [2004]).

[6] *Blunier et al.* [1998] and *Blunier and Brook* [2001] synchronized ice core records from Antarctica and Greenland using variations in the concentration of atmospheric methane (a globally well-mixed gas) in air bubbles enclosed within the ice. This work showed that D-O events in Greenland correspond to at least four slower, smaller (relative to Greenland) changes in Antarctica. The onsets of the Bond cycles in Greenland correspond to the warmest peaks in Antarctic temperature (Antarctic events A1–A4), followed by more subdued variability (Figure 1) [*Stocker and Johnsen*, 2003; *EPICA Community Members*, 2006]. This subdued variability has been controversial because the magnitude of the temperature change was only ambiguously resolved in the Byrd ice core [*Johnsen et al.*, 1972; *Blunier et al.*, 1998; *Blunier and Brook*, 2001]. *Stocker and Johnsen* [2003], *Knutti et al.* [2004], and *Siddall et al.* [2006a] used variations on a simple model which assumed a lagged, opposite response in Antarctic temperature to Greenland temperature changes. This work found that the Byrd temperature proxy record was consistent with the assertion that the shorter D-O events correspond to periods of warming and cooling in Antarctica, despite being poorly resolved. Recent results from the EPICA Dronning Maud Land [*EPICA Community Members*, 2006] ice core support this conclusion by unambiguously resolving the low-magnitude temperature variability which is suggested to correspond to periods of shorter D-O events and demonstrating a robust, linear relationship between the duration of D-O cold stadial periods and Antarctic warming. We will refer to the ensemble of Antarctic temperature variability during MIS 3 as AA variability. AA variability has also been referred to as the “southern response” or “southern mode” [*Alley and Clark*, 1999; *Clark et al.*, 2002, 2007].

[7] The relative timing between climate fluctuations of the northern and southern high latitudes, as inferred from the methane synchronization [*Blunier et al.*, 1998; *Blunier and Brook*, 2001], has also been observed between planktic (D-O-like variability) and benthic foraminiferal stable oxygen isotope ratios (Antarctic (AA)-like variability) in a single set of samples from marine sediment core MD95-2042 from 3142 m water depth on the Portuguese margin (Figure 1) [*Shackleton et al.*, 2000]. Similar millennial variability appears to be a robust phenomenon within the

TABLE 1. Summary of the Sea Level Reconstructions Discussed in the Text and Their Stratigraphic Characteristics

Data Type	Reference	Description (Core Name, Location, and Water Depth)	Higher at the Start of MIS 3 Than End?	Fluctuations	Magnitude
Benthic oxygen isotopes (individual)	<i>Shackleton</i> [1987]	V19-30; 3°23'S, 83°31'W; 3091 m; western equatorial Pacific	yes	4+	20 m
	<i>Labeyrie et al.</i> [1987]	V19-30; 3°23'S, 83°31'W; 3091 m; western equatorial Pacific	yes	4	20–30 m
	<i>Ninnemann et al.</i> [1999]	TN057-21; 41°8'S, 7°49'E; 4981 m; Cape Basin (southeast Atlantic)	yes	3+	20–30 m
	<i>Shackleton et al.</i> [2000]	MD95-2042; 37°47.99'N, 10°9.99'W; 3146 m; Portuguese Margin	yes	4	20–40 m
	<i>Pahnke et al.</i> [2003]	MD97-2120; 45.53°S, 174.93°W; 1210 m; Chatham Rise (southwest Pacific)	yes	4	20–40 m
Benthic oxygen isotopes (stacks)	<i>Lisiecki and Raymo</i> [2005]	stack of 57 globally distributed records, synchronized using graphical correlation	yes	4	20 m
	<i>Martinson et al.</i> [1987]	Mapping Spectral Variability in Global Climate Project benthic isotope stack of records from around the globe, synchronized using insolation record	yes	3+	20 m
	<i>Huybers and Wunsch</i> [2004]	benthic stack based on the leading empirical orthogonal function of five benthic records, age model assumes constant sedimentation for last 17 glacial cycles	yes	4	20–30 m
Planktic oxygen isotopes	<i>Linsley</i> [1996]	ODP769; 8.78°N, 121.29°E; Sulu Sea, eastern equatorial Pacific	yes	3+	20–30 m
	<i>Dannenmann et al.</i> [2003]	IMAGES97-2141; 8.8°N, 121.3°E; Sulu Sea, eastern equatorial Pacific	yes	4+	20–30 m
	<i>Lea et al.</i> [2002]	TR163-19; 2.15°N, 90.57°W; western equatorial Pacific	no	4	20–40 m
Red Sea	<i>Siddall et al.</i> [2003]	GeoTueKL11; 18°44.5'N, 39°20.6'E; central Red Sea planktic isotopes	yes	4	30–40 m
	<i>Arz et al.</i> [2007]	GeoB 5844-2; 27°42.81'N, 34°40.9'E; 963 m; northern Red Sea benthic isotopes	yes	4	20–30 m
Combined methods	<i>Cutler et al.</i> [2003]	V19-30; 3°23'S, 83°31'W; 3091 m; western equatorial Pacific, benthic isotope record scaled to coral indicators of sea level	yes	3+	30–40 m
	<i>Waelbroeck et al.</i> [2002]	benthic isotope records scaled to coral indicators of sea level	yes	4	20 m
	<i>Shackleton</i> [2000]	assumptions about the Dole effect and deep water temperatures used to generate a record of global ice volume/sea level variations from the V19-30 benthic isotope record and the Vostok Deuterium record [ <i>Petit et al.</i> , 1999]	yes	4	20–40 m
Fossil coral reefs	<i>Chappell</i> [2002]	Huon Peninsula; 6.42°S, 147.5°E; raised fossil reef terrace, U/Th ages and reef growth model with stratigraphy	yes	4	10–20 m
	<i>Thompson and Goldstein</i> [2005, 2006]	Huon Peninsula; 6.42°S, 147.5°E; U/Th ages on corals corrected for open system effects	yes	4+	20–30 m

climate system, occurring over multiple periods in the past linked to periods when the ice sheets were of intermediate size, smaller than the glacial maximum ice sheets, yet larger than interglacial ice sheets [*Oppo et al.*, 1998; *McManus et al.*, 1999; *Siddall et al.*, 2007]. Observations place this “intermediate” range of ice volume at the equivalent of 40–100 m of global sea level lowering [*Siddall et al.*, 2007]. *Clark et al.* [2001] explore a possible link between sea level and millennial variability by exploring the effect of the southward extent of the Laurentide ice sheet and the routing of meltwater, which in turn provides a control on the

transport of heat in the surface waters of the Atlantic (i.e., the Atlantic Meridional Overturning Circulation, see section 1.3).

### 1.3. Mechanisms of Millennial Climate Change

[8] D-O variability during MIS 3 occurs on millennial time scales and so cannot be directly explained by orbital forcing. Current concepts instead link the D-O variability to other external forcing and/or to internal processes within the Earth’s climate system. Some authors have suggested that D-O variability follows a regular ~1500-year period [*Bond et al.*, 1997; *Mayewski et al.*, 1997; *Alley et al.*, 2001;

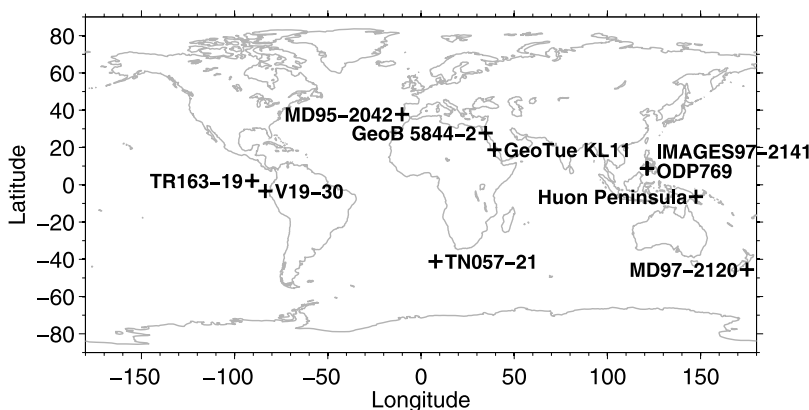


**Figure 2.** Locations of the sea level reconstructions used in this paper and listed in Table 1.

Schulz, 2002; Rahmstorf, 2003]. Studies have ascribed this regularity to solar output variability, but, as yet, there is little evidence for solar variability on a  $\sim 1500$ -year period [Stuiver and Braziunas, 1993; Bard and Frank, 2006], although it might arise as a multiple of shorter-period solar variability [e.g., Bond et al., 2001; Braun et al., 2005]. The large, apparently quasi-regular variability has been ascribed to stochastic resonance within the Earth's climate system in order to explain the fact that the periodicity may not always be 1500 years but may sometimes be multiples of 1500 years [Alley et al., 2001; Rahmstorf and Alley, 2002; Ganopolski and Rahmstorf, 2001]. However, other work argues that there is no  $\sim 1500$ -year periodicity [e.g., Wunsch, 2000; Ditlevsen et al., 2005]. Alternative explanations focus on mechanisms internal to the Earth system, paced more loosely by factors such as the heat storage capacity of the Southern Ocean and the residence time of deep water masses in the ocean [e.g., Dansgaard et al., 1984; Broecker et al., 1985; Stocker et al., 1992; Schiller et al., 1997; Stocker and Johnsen, 2003]. Ditlevsen [1999] and Ditlevsen et al. [2005] suggest that the abrupt variability is due entirely to noise in the climate system, for example, via erratic meltwater releases from the margins of the large continental ice sheets [e.g., Clark et al., 2001]. It is clear that there is no consensus regarding the regularity of D-O events and the underlying mechanisms. One of the key aspects that is unconstrained in this discussion concerns the timing and behavior of global sea level variability, both as a measure of ice sheet growth and decay and as a measure of freshwater extraction from, and addition to, the world ocean. This is discussed in the following paragraphs.

[9] A wide range of modeling studies over the last decades [e.g., Stocker et al. 1992; Manabe and Stouffer, 1997; Ganopolski and Rahmstorf, 2001; Stocker and Johnsen, 2003; Knutti et al., 2004; Schmittner, 2005] indicate that a flux of freshwater into the North Atlantic strongly affects the oceanic northward heat transport associated with the Atlantic Meridional Overturning Circulation (AMOC). (The AMOC is the large-scale transport of salt and heat in

the Atlantic by the wind and density-driven circulation. Density-driven circulation results from high-latitude cooling and salt rejection during sea ice formation, which generates dense water masses at the surface and thereby oceanic convection. This density-driven circulation may be sensitive to freshwater input, which reduces the surface density, preventing convection.) The large Northern Hemisphere ice sheets are a major potential source of freshwater to the North Atlantic, either via iceberg calving events or in the form of meltwater events [e.g., Clark et al., 1999].

[10] Major iceberg calving events are known as “Heinrich events,” which are marked by Heinrich layers of IRD across large areas of the North Atlantic (as first described by Heinrich [1988]). “Heinrich events” coincide with the D-O stadials at the conclusion of the Bond cycles (see Hemming [2004] for a review). Estimates for the freshwater input to the North Atlantic associated with Heinrich events vary between 2 and 15 m of sea level equivalent ice volume [Chappell, 2002; Hemming, 2004; Roche et al., 2004; Rohling et al., 2004]. Whether or not the actual figure is 2 or 15 m of sea level equivalent ice volume, Heinrich events provide an unambiguous indication of substantial (iceberg) meltwater release into the North Atlantic and have formed an impetus for modeling studies to consider freshwater pulses as a trigger for D-O variability (see Flückiger et al. [2006] for a review).

[11] Some workers, however, question the importance of the AMOC's northward heat transport for the temperature variability around the North Atlantic and instead focus more on changes in the zonality of atmospheric circulation over the North Atlantic (for overviews, see Seager et al. [2002] and Seager and Battisti [2007]). As alternatives to the effects of Heinrich events on high-latitude convection as a trigger for D-O variability, other studies have concentrated on mechanisms that center on shifts in the main locus of deep water formation. These include atmospheric freshwater transport between the Atlantic and Pacific [Leduc et al., 2007], insulation of the surface ocean by sea ice [e.g., Li et al., 2005], and local Nordic Sea freshwater forcing from meltwater and ice rafting [Lekens et al., 2006]. The significance of the seasonal imprint of different mechanisms for

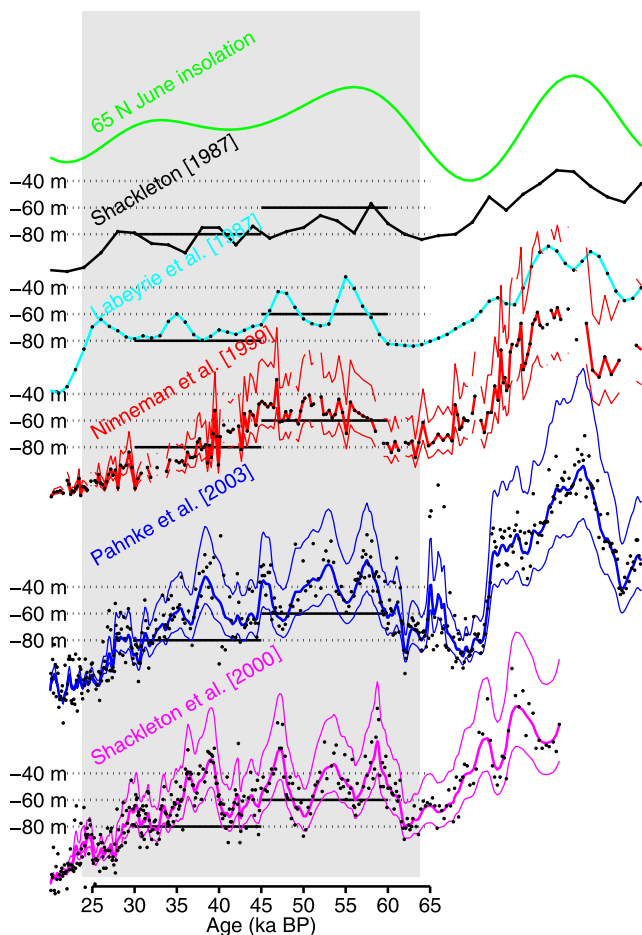


**Figure 3.** Sea level estimates from benthic oxygen isotope records as discussed in section 2.2. MIS 3 (60–25 ka B.P.) is in gray, and black dots are data points. Black lines are at –60 and –80 m and indicate “typical” estimates for the early and late periods of MIS 3, respectively. Where single lines are shown, no uncertainty margin was given in the original text but is of the order of  $\pm 30$  m [see, e.g., Siddall et al., 2006c]. Where multiple lines are shown, we have estimated sea level on the basis of the suggested calibration of Adkins et al. [2002]; the uncertainty is due to the variation in this scaling between different ocean basins, as discussed in section 2.2.

the ice core temperature record and ice sheet mass balance is discussed by Denton et al. [2005]. Depending on the model in question, either D-O stadials or interstadials are considered to be the “perturbed” or “agitated” states in the system [Ganopolski and Rahmstorf, 2001; Stocker and Johnsen, 2003]. In an alternative view, the MIS 3 climate may have been permanently in a state of disequilibrium [Ditlevsen, 1999; Ditlevsen et al., 2005].

[12] In order to understand abrupt climate changes during MIS 3 we must establish whether the ice sheets have an active involvement, act as trigger or amplifier, or merely respond in a passive manner (i.e., as an integrated response to the temperature changes over the duration of Bond cycles or AA climate events). Careful assessment of the magnitude

and phasing of global ice volume fluctuations within MIS 3 will help us to achieve this goal.

## 2. STABLE OXYGEN ISOTOPE RATIOS

[13] Stable oxygen isotope ratios measured on fossil calcite tests of unicellular zooplankton and benthos (foraminifera) are widely accepted as an approximate indicator of long-term variations in global ice volume (hence eustatic sea level). The purpose of including these records here is to begin to build a general picture of MIS 3 sea level variations, rather than to consider absolute values.

### 2.1. Using Stable Oxygen Isotope Records to Infer Sea Level Change

[14] Rohling and Cooke [1999] provide a general review of stable oxygen isotope fractionation in the Earth system, and we here summarize only the aspects relevant to the problem at hand. Compared to  $^{18}\text{O}$ , the lighter  $^{16}\text{O}$  isotope is preferentially evaporated from the ocean. In turn, Rayleigh distillation in the atmosphere causes strong relative enrichment of  $^{16}\text{O}$  in high-latitude precipitation [Dansgaard, 1964]. During glacial periods, growth of the large continental ice sheets leads to an increase of the  $^{18}\text{O}/^{16}\text{O}$  ratio in ocean water because more of the global inventory of  $^{16}\text{O}$  becomes contained in the ice sheets. In this way the oxygen isotope ratio in foraminifera is sensitive to global ice volume. However, this representation is complicated by variability of isotope ratios within the oceans due to differences in the evaporation and precipitation influences on surface water isotope ratios, advection and mixing of water masses from different source regions (with different isotopic signatures), and the temperature-dependent isotope fractionation between the water in which the foraminifera live and deposit their carbonates shells [e.g., Shackleton and Opdyke, 1973; Rohling and Bigg, 1998; Schmidt, 1999; Lea et al., 2002; Wadley et al., 2002; Waelbroeck et al., 2002].

[15] If the mean isotopic composition of the ice caps remained constant while they changed in size and if the temperature variations were known and the water mass structure of the oceans was constant, sea level could be accurately estimated from marine isotope records. In practice, the ice composition and ocean structure are usually assumed to be constant, and then sea level is estimated after subtraction of a temperature effect, which may be either measured or hypothesized [Shackleton, 1987]. Glacial to interglacial variation in oxygen isotope ratios in water, as measured on pore waters in marine sediment cores, suggests some degree of spatial heterogeneity between ocean basins within a range of 0.7–1.3‰ [Adkins et al., 2002]. Because the observations include the Pacific Ocean, the Southern Ocean, and the Atlantic Ocean we assume that this should reasonably capture the range of possible values within ocean basins and around the globe.

[16] We present stable oxygen isotope records for deep-sea benthic and planktic foraminifera from sediment cores recovered at a variety of locations in the world ocean.

Where the records have not been explicitly scaled to sea level in the literature, we take the range of measured relationships between oxygen isotopes and sea level found by *Adkins et al.* [2002]. Specifically, we take a middle value of 1‰ for 120 m sea level change, use values of 0.7 and 1.3‰ for 120 m sea level change to indicate uncertainties to our estimate, and normalize the records to an Last Glacial Maximum (LGM) sea level of 120 m below the present [*Fairbanks, 1989; Peltier and Fairbanks, 2006*]. We normalize the records by fixing the mean value of the records during the LGM period (defined by the peak in the benthic oxygen isotope values around 19–21 ka B.P.) to 120 m below present. There is some disagreement in the literature over the level of the LGM lowstand (–120 m [*Fairbanks, 1989; Peltier and Fairbanks, 2006*] or –135 m [*Yokoyama et al., 2000*]). Here we are most interested in the variability of sea level during MIS 3. The chosen LGM sea level value has no impact on our conclusions regarding sea level fluctuations during MIS 3. However, the absolute estimates may be as much as 15 m above the real values if the lowstand reached –135 m, rather than the –120 m we assume here.

[17] Following the work of *Adkins et al.* [2002] and *Adkins and Schrag* [2003] we assume that deep ocean temperatures approached the freezing point of seawater during the glacial period and were therefore relatively constant. This assumption requires that there is a transition in deep ocean mean temperature between glacial and interglacial periods of 2°C [*Chappell and Shackleton, 1986; Cutler et al., 2003*]. We are only interested in sea level fluctuations during MIS 3, and therefore our approach does not account for this implied transition in deep ocean temperatures. Consequently, it greatly overestimates the sea level highstands of the peak interglacials MIS 5e and MIS 1. However, the approach seems valid through MIS 3, as witnessed by agreement with sea level indicators from fossil coral reefs, and a similar approach has been followed previously [e.g., *Chappell and Shackleton, 1986; Cutler et al., 2003*].

[18] Reproducibility of replicate oxygen isotope analyses is typically less than 0.1‰ [e.g., *Rohling and Cooke, 1999*], which is equivalent to between 9 and 17 m. This does not represent the complete uncertainty in interpreting the oxygen isotope ratios in terms of sea level because of the effects of temperature and hydrographic changes on the record. For example, a 1°C change in temperature is equivalent to a 0.26‰ change in oxygen isotope ratios [*Kim and O’Neil, 1997*], or between 24 and 45 m of sea level change. Evidently, the benthic isotopes should be considered predominantly as a qualitative measure of ice volume change.

[19] More sophisticated methods of inferring sea level records from benthic oxygen isotope records have also been used. For example, *Bintanja et al.* [2005] used an ice sheet model coupled to a model of benthic isotope fractionation to derive both sea level and high-latitude temperature with some success. By using a stacked benthic isotope record and considering individual as well as stacked isotope records, the approach of *Bintanja et al.* [2005] takes tentative steps

to account for the hydrographic differences between ocean basins which affect the benthic oxygen isotope record.

[20] Because we are attempting to better understand the common stratigraphy of the benthic oxygen isotope records, we opt for the simple approach described here and concentrate only on the broad common features in the various records considered. We then make further comparisons with more sophisticated approaches such as that outlined by *Bintanja et al.* [2005]. These features are briefly outlined in section 2.2.

## 2.2. Benthic Foraminiferal Oxygen Isotope Records

[21] Isotope records from benthic foraminifera dominate the study of ice volume/sea level at longer time scales because planktic records from the surface ocean are subject to greater variations of the oxygen isotope ratio than benthic records from the deep ocean because of much greater temperature variability and regional variations in the freshwater budget [e.g., *Rohling and Bigg, 1998; Wadley et al., 2002*]. However, in the case of benthic foraminifera, there normally are only very low numbers of suitable specimens for analysis per unit sample volume in deep-sea sediments because of depth-dependent reduction of the organic (i.e., food) flux to the seafloor. As a consequence, there exist only a handful of benthic records with adequate resolution to unambiguously resolve the variability within MIS 3, but this number is steadily increasing.

[22] *Labeyrie et al.* [1987] and *Shackleton* [1987] outlined two early approaches to reconstruct an oxygen isotope record representative of the fluctuations in global mean sea level (and so, by approximation, in global ice volume).

[23] Figure 3 shows the sea level reconstruction of *Labeyrie et al.* [1987]. These authors argued that the temperature of glacial deep water in the Norwegian Sea was relatively constant throughout the glacial cycle (including interglacial periods) because temperatures there are currently close to the freezing point of water there. Unfortunately, there were sections with few or no foraminifera in the Norwegian Sea cores. The deep Pacific was relatively stable with respect to water mass and temperature fluctuations (i.e., temperatures approached freezing point) only during the glacial periods. Thus, an argument was constructed that the two study areas suffered only minimal temperature fluctuations during different periods, when isotope records would primarily reflect ice volume variations. In order to minimize temperature effects through the glacial cycle and provide a complete record through the glacial cycle, Norwegian Sea cores were used to reconstruct interglacial variations, and equatorial Pacific core V19-30 was used to reconstruct glacial variations.

[24] *Chappell and Shackleton* [1986] and *Shackleton* [1987] also used the benthic oxygen isotope record of equatorial Pacific core V19-30, but combined it with sea level estimates from fossil coral terraces on Huon Peninsula (Figure 3, see also sections 3.1 and 5.3). They found that a simple linear scaling of the V19-30 benthic oxygen isotope record between a modern interglacial sea level of 0 m and a full glacial sea level at –120 m failed to explain the

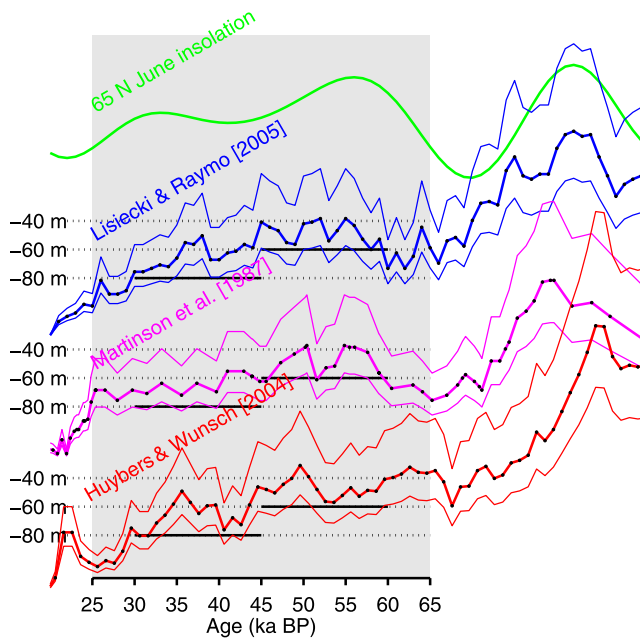


**Figure 4.** Sea level estimates from stacked benthic oxygen isotope records as discussed in section 2.2. MIS 3 (60–25 ka B.P.) is in gray, and black dots are data points. Black lines are at  $-60$  and  $-80$  m and indicate “typical” estimates for the early and late periods of MIS 3, respectively. Where single lines are shown, no uncertainty margin was given in the original text but is of the order of  $\pm 30$  m [see, e.g., Siddall et al., 2006c]. Where multiple lines are shown, we have estimated sea level on the basis of the suggested calibration of Adkins et al. [2002]; the uncertainty is due to the variation in this scaling between different ocean basins, as discussed in section 2.2.

magnitude of variability found in the Huon Peninsula record. However, if a  $2^{\circ}\text{C}$  cooling of the deep ocean during glacial periods was assumed, relative to interglacial periods, then the two sets of data could be aligned. A reconstruction of deep ocean temperature based on a comparison between stable oxygen isotope measurements of pore waters and benthic foraminifera from deep sea cores has confirmed that the glacial deep ocean was indeed a couple of degrees cooler than today [Adkins et al., 2002].

[25] Figure 3 also shows another important benthic foraminiferal oxygen isotope record, namely, that of core TN057-21 from 4981 m water depth in the Cape Basin (southeast Atlantic) [Ninnemann et al., 1999]. The site of TN057-21 is bathed in Antarctic Bottom Water (AABW), which originates in the Weddell Sea near to the freezing point of seawater. If this was also the case in the past, then the water temperature at this site may have been relatively stable during MIS 3, in which case the isotope record would reflect a relatively unbiased form of the ice volume effect. This is why we include this record here. We consider that temperature bias may not be fully excluded because of an element of Circumpolar Deep Water/lower North Atlantic Deep Water (NADW) entrainment in the Antarctic Bottom Water (AABW) that bathes the core site. Indeed the glacial to interglacial change in the oxygen isotope record is  $1.7\text{‰}$ ,

greater than the range of  $0.7\text{‰}$ – $1.3\text{‰}$  that can be attributed to the glacial to interglacial ice volume component [Adkins et al., 2002]. This would suggest that there indeed are additional factors such as deep ocean mixing affecting the TN057-21 benthic isotope record. Unfortunately, this record does not fully resolve the MIS 3 sea level variability. It nevertheless points to the importance of taking more benthic oxygen isotope records in the Southern Ocean in the future.

[26] Two key high-resolution benthic foraminiferal oxygen isotope records are particularly important to understanding MIS 3 sea level variability (Figure 3). The first is that of core MD95-2042 from 3142 m depth on the Iberian margin (NE Atlantic) [Shackleton et al., 2000]. As mentioned before, the isotope records for this core have offered direct and unambiguous insight into the phase relationship between the surface water planktic (D-O-style) variability and the deep-sea benthic (AA-style) variability at this site, which may offer the best available chronological control on the timing of deep-sea stable oxygen isotope fluctuations in North Atlantic deep waters. The other key record is that of core MD97-2120 from 1210 m depth on Chatham Rise (SW Pacific) [Pahnke et al., 2003; Pahnke and Zahn, 2005]. Despite the recovery from almost antipodal sites at vastly different depths in completely different ocean basins with entirely different water mass structures and from entirely different water masses (lower NADW/AABW boundary and lower Antarctic Intermediate Water (AAIW), respectively), the benthic foraminiferal oxygen isotope records of MD95-2042 and MD97-2120 display extremely similar signals, although a phase shift of several thousand years between these two records cannot be excluded [Skinner and Shackleton, 2005]. Displayed in Figure 3 using the same scaling as applied to the other benthic stable oxygen isotope records, this structure displays four fluctuations equivalent to  $20\text{--}40$  m sea level magnitude within MIS 3.

[27] Finally, we consider so-called “stacked” benthic foraminiferal oxygen isotope records, which are statistical compilations of several (to many) individual records. These records are shown in Figure 4 and are of interest because the stacking procedure should help to filter out more local hydrographic variability in favor of the underlying general (global) changes. Martinson et al. [1987] presented the first widely used (Mapping Spectral Variability in Global Climate Project (SPECMAP)) stack of benthic isotope records, based on benthic records from around the globe on time scales that were synchronized by tuning to the orbital insolation record. Huybers and Wunsch [2004] create their independent benthic stack on the basis of the leading empirical orthogonal function of five benthic records on an age model that assumes a constant sedimentation rate over the last 17 glacial cycles. Note that four of these five records are from the Atlantic, and so this stack may be biased toward the larger responses found in this basin [e.g., Waelbroeck et al., 2002]. Lisiecki and Raymo [2005] created a stack of 57 globally distributed benthic records, which were synchronized using a graphic correlation technique.

[28] Figures 3 and 4 and Table 1 allow comparison of all the aforementioned benthic records, which we have scaled

to sea level using the procedure outlined above. The horizontal black lines in the plots lie at the same sea level on each curve ( $-60$  and  $-80$  m) to facilitate visual inspection of the records and will be used throughout the paper. Visual inspection is used to establish sea level estimates from the records throughout this paper. The maxima and minima of a single fluctuation are defined by at least three points for oxygen-isotope-based records and by single coral estimates. The black lines are spaced at 20 m intervals so that fluctuations in the range of 20–40 m are easy to read off the plots without overinterpreting the records. If the magnitude of the variability is cited as a range, then this refers to the range of multiple fluctuations. On studying the plots in Figures 3 and 4, common stratigraphic characteristics of the underlying MIS 3 sea level record immediately emerge. MIS 3 is sandwiched between periods of generally lower sea level (MIS 4 and MIS 2). Following MIS 4 (approximately  $-80$  to  $-90$  m), the records show a sea level rise of 20–40 m into MIS 3. Next, sea level is seen to stand  $\sim 20$  m higher during the first half of MIS 3 (approximately  $-60$  m) than during the later part (approximately  $-80$  m). Possibly, the higher sea level during the first part of MIS 3 is a response to the increased summer insolation at  $65^\circ\text{N}$  during that time (Figures 3 and 4), although an alternative explanation will be discussed in section 6.5. Following MIS 3, sea level falls to  $-120$  or  $-135$  m during MIS 2 [Fairbanks, 1989; Rohling et al., 1998; Yokoyama et al., 2000; Peltier and Fairbanks, 2006]. These stratigraphic characteristics are common to MIS 3 sea level reconstructions from many different techniques, as shown by the various records collected in this paper.

[29] Figure 3 allows a first evaluation of any signs of millennial variability in the individual records, and it is immediately evident that all records do contain some signal structure within MIS 3. The record of Shackleton [1987] does not clearly resolve this variability but may contain four or five fluctuations of the order of 20 m magnitude. The Labeyrie et al. [1987] record contains four fluctuations of between 20 and 30 m magnitude. The Ninnemann et al. [1999] Southern Ocean record is noisy, but the noise has a magnitude of 10–30 m (i.e., a similar magnitude to the other benthic isotope estimates). Both the records of Shackleton et al. [2000] and Pahnke et al. [2003] clearly resolve four fluctuations of between 20 and 40 m magnitude, which are stratigraphically very similar to each other.

[30] Stacked benthic oxygen isotope records may to some extent remove the hydrographic variations that could distort any individual sea level record from a single core. None of the stacked records reproduced in Figure 4 have considered millennial-scale variability during synchronization of the individual contributing records, so that the stacked records may be expected to represent any millennial-scale variability in a smoothed manner (except perhaps the Lisiecki and Raymo [2005] record, see below), or indeed to remove it if the records stack the sea level fluctuations “out of phase.” Despite this statistical smoothing effect, all stacked records show distinct variability within MIS 3. The Martinson et al. [1987] stack shows two major fluctuations in the early part

of MIS 3 of between 10 and 30 m magnitude, while the Huybers and Wunsch [2004] record picks out three fluctuations with magnitudes of  $\sim 30$  m. However, we do have some reservations about the Huybers and Wunsch [2004] record on these short time scales because the stacking method used has removed any obvious signal of the MIS 4 lowstand (possibly because the records have been stacked “out of phase” during this period). Given that the Lisiecki and Raymo [2005] stack was constructed using a graphic correlation tool to synchronize the individual records, it may be the most likely to retain a relatively unsmoothed representation of any millennial-scale variability. Within MIS 3, this record shows four fluctuations with magnitudes between 10 and 30 m.

### 2.3. Planktic Foraminiferal Oxygen Isotope Records

[31] Figure 5 shows a high-resolution planktic oxygen isotope record from the Sulu Sea in the equatorial Pacific [Linsley, 1996]. The Sulu Sea is a relatively isolated region in the western equatorial Pacific, characterized by a net input of freshwater due to high runoff from SE Asia and nearby islands, which may considerably affect oxygen isotope ratios in the surface waters. To some extent, the impact of the Sulu Sea’s freshwater balance on its surface water oxygen isotope ratios is related to sea-level-modulated changes in the exchange of water in the basin with the open ocean through the connecting straits, but (given the large catchment area) changes in the actual balance between evaporation and precipitation/runoff are also likely to be significant.

[32] The Sulu Sea record reveals glacial to interglacial oxygen isotope variations of a similar order ( $\sim 1.2\text{‰}$ ) to that anticipated for the global mean [Linsley, 1996]. Initially, it was therefore interpreted directly in terms of ice volume variations [Linsley, 1996]. More recent work involving Sulu Sea records, using Mg/Ca-based temperature estimates, has endeavored to remove the influence of any temperature fluctuations to derive records of the oxygen isotope ratio of the water mass in which the foraminiferal tests had formed [Dannenmann et al., 2003] and to thus reveal the ice volume effect and any superimposed local hydrographic and freshwater budget effects. Figure 5 compares the Linsley [1996] and Dannenmann et al. [2003] records for the Sulu Sea. Both contain a good deal of noise, which likely reflects variations in evaporation and precipitation/runoff from the catchment areas that drain into the basin (i.e., local hydrological influences). Underlying the noise, the records show generally lighter isotope ratios, perhaps relating to higher sea level, during the early part of MIS 3 than during the later stages of MIS 3. The five-point Gaussian-smoothed record of Dannenmann et al. [2003] suggests four or five millennial-scale fluctuations within MIS 3 that would be equivalent to sea level changes of 20–40 m magnitude.

[33] Lea et al. [2002] investigated core TR163-19 from Cocos Ridge, north of the Galapagos Islands in the eastern equatorial Pacific, and used Mg/Ca measurements to remove temperature effects from their record. The resulting



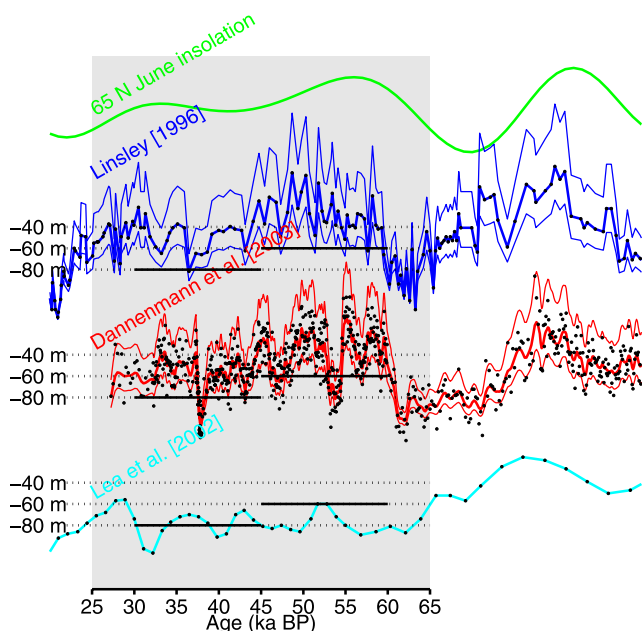


**Figure 5.** Sea level estimates from planktic oxygen isotope records. MIS 3 (60–25 ka B.P.) is in gray, and black dots are data points. Black lines are at  $-60$  and  $-80$  m and indicate “typical” estimates for the early and late periods of MIS 3, respectively. The error on the *Lea et al.* [2002] estimate is somewhat less than  $\pm 30$  m [see, e.g., *Siddall et al.*, 2006c], given that variation in temperature is taken into account. Where multiple lines are shown, we have estimated sea level on the basis of the suggested calibration of *Adkins et al.* [2002]; the uncertainty is due to the variation in this scaling between different ocean basins, as discussed in section 2.3.

record of surface water oxygen isotope ratios is shown in Figure 5. *Lea et al.* [2002] noted that this record displays some similarity to the benthic foraminiferal oxygen isotope record of *Labeyrie et al.* [1987] (Figure 3); both suggest four sea level fluctuations of 20–30 m magnitude and include a peak in sea level at the end of MIS 3.

#### 2.4. Red Sea Residence Time Method

[34] Oxygen isotope ratios in the Red Sea are highly sensitive to changes in sea level and give an additional means to derive sea level estimates during MIS 3. We discuss this approach below.

[35] The Red Sea is subject to strong net evaporation. Evaporation strongly enhances oxygen isotope ratios in marginal basins that are restricted from the open ocean by a small strait with a shallow sill, such as the Red Sea (and the Mediterranean [*Rohling*, 1999]), because enhancement of oxygen isotope ratios in the basin is linked not only to the rate of evaporation but also to the refreshment rate of water in the basin by exchange over the sill (the residence time of water in the basin). The longer the residence time, the longer the water is exposed to the high evaporation rates, and the heavier the isotope ratio becomes because of preferential removal of the lighter  $^{16}\text{O}$  isotope by evaporation.

[36] The Red Sea is separated from the open ocean by the Hanish Sill, which is only 137 m deep [*Werner and Lange*, 1975; *Rohling et al.*, 1998; *Fenton et al.*, 2000; *Siddall et al.*, 2002, 2003, 2004], which is not much deeper than the depth of a full glacial lowstand (120 m) [*Fairbanks*, 1989; *Peltier and Fairbanks*, 2006]. Modeling results indicate that glacioisostatic effects on the sill may lower the sill position by a maximum of 17 m during periods of glacial maxima [*Siddall et al.*, 2004]. As noted by *Rohling et al.* [1998] and *Siddall et al.* [2003, 2004], there likely is a gradual (very small) sill uplift. This very limited sill uplift means that the sill has remained submerged during at least the last 500,000 years, even in the most extreme glacial lowstands [*Rohling et al.*, 1998; *Siddall et al.*, 2003, 2004; *Fernandes et al.*, 2006]. Bathymetric data show that the sill passage narrows from 110 km at modern sea level to around 6 km at  $-120$  m. This reduction of the width of the sill passage with depth causes an exponential decrease in the sill passage area over almost three orders of magnitude by full glacial sea level lowering, which in turn means that (even today) the restricted exchange of waters between the Red Sea and the open ocean is extremely sensitive to sea level. This strong reduction of cross-sectional area with respect to sea level is illustrated in Figure 6.

[37] In summary, the enhancement of oxygen isotope ratios by evaporation and the great sensitivity of this enhancement to exchange over the sill (which critically depends on sea level as the first-order cause of change in the area of the sill passage (Figure 6)) strongly links Red Sea oxygen isotope ratios with sea level. This strong linkage is best exemplified by the fact that the full glacial-interglacial range of change in stable oxygen isotope ratios is 5.5–6‰, versus roughly 1–1.2‰ in the open ocean [*Thunell et al.*, 1988; *Hemleben et al.*, 1996; *Rohling et al.*, 1998; *Fenton et al.*, 2000; *Siddall et al.*, 2003; *Arz et al.*, 2003a].

[38] The residence time effect in the Red Sea also affects salinity in the basin; in fact, this salinity effect was studied before the accompanying impact on the oxygen isotopes. It was found that the times of full glacial sea level lowstands

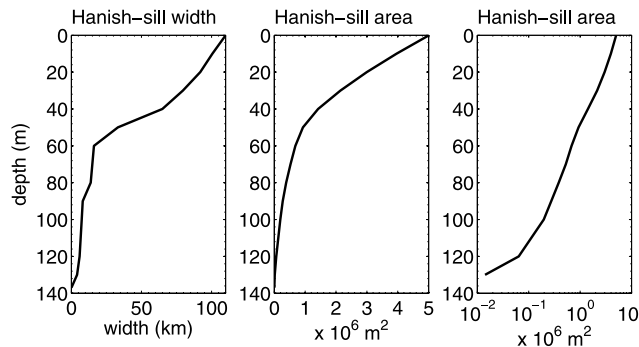


**Figure 6.** The width and cross-sectional area of Hanish Sill with respect to water depth. Note the large change in the cross section in the 0–120 m range of glacial to interglacial sea level. That the cross section changes by nearly three orders of magnitude over this range is one of the key reasons that the Red Sea is so sensitive to sea level change.

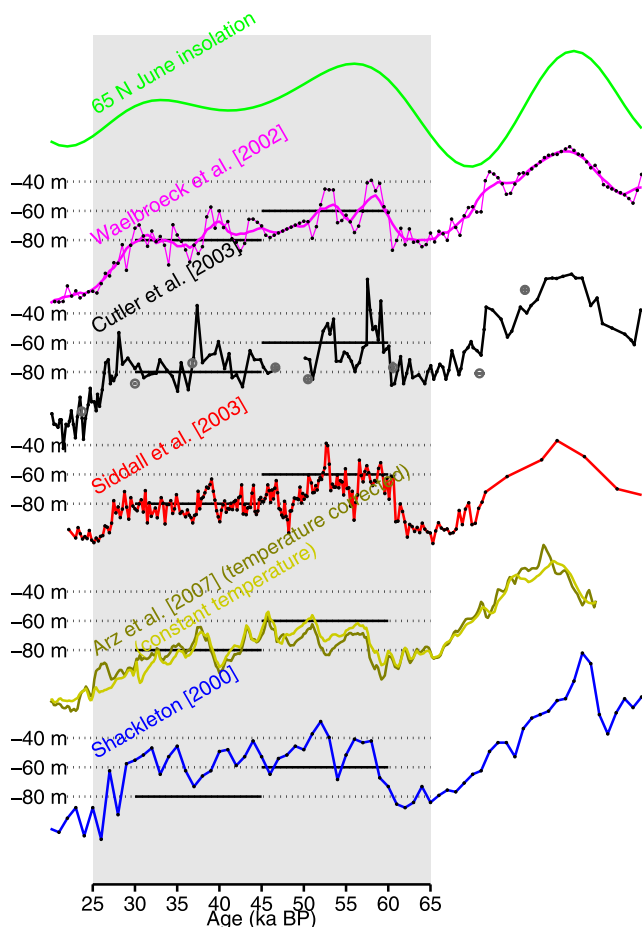


**Figure 7.** Modeled/marginal basin records. MIS 3 (60–25 ka B.P.) is in gray, and black dots are data points. Black lines are at  $-60$  and  $-80$  m and indicate “typical” estimates for the early and late periods of MIS 3, respectively. Errors in some of the techniques are shown on the plot. The sensitivities of the other methods are  $\pm 13$  m [Waelbroeck et al., 2002],  $\pm 12$  m [Siddall et al., 2003], and  $\pm 12$  m (without temperature correction) and  $\pm 8$  m (with temperature correction) [Arz et al., 2007]; Shackleton [2000] gives no uncertainty, but it may be assumed that this is in the range of  $\pm 30$  m [Siddall et al., 2006c]. Note that the Waelbroeck et al. [2002] reconstruction is shown here on the same time orbital scale as the Shackleton [1987] V19-30 benthic isotope record. The coral data used to scale the estimates of Cutler et al. [2003] are shown next to that curve as circles.

were characterized by hypersaline conditions in the Red Sea, which caused development of chemical precipitates, benthic foraminiferal faunas indicative of very high salinities, and aplanktic zones [e.g., Milliman et al., 1969; Deuser et al., 1976; Ivanova, 1985; Winter et al., 1983; Reiss et al., 1980; Locke and Thunell, 1988; Thunell et al., 1988; Almogi-Labin et al., 1991; Rohling, 1994; Hemleben et al., 1996; Rohling et al., 1998; Fenton et al., 2000]. Aplanktic zones are intervals during which basin salinities in excess of 49 PSU caused widespread (local) extinction of planktic foraminifera, when sea level stood below about  $-100$  m (for an overview, see Fenton et al. [2000]). Rohling

et al. [1998] used such evidence of species diversity from the central Red Sea with a crude hydraulic control approximation for water exchange across the sill, to estimate the magnitudes of sea level lowstands during the last five glacial maxima (MIS 2, 6, 8, 10, and 12). An improved and expanded version of this approach realized the potential of Red Sea oxygen isotope data to quantify continuous records of sea level change [Siddall et al., 2003, 2004, 2006b].

[39] Siddall et al. [2003] combined a three-layer hydraulic model to calculate water mass exchange at the sill [Siddall et al., 2002] with a model of oxygen isotope fractionation in an evaporative basin developed for the Mediterranean [Rohling, 1999]. By varying the sill depth in the model and assuming a  $5^{\circ}\text{C}$  temperature drop at the LGM, a relationship was calculated between sea level and oxygen isotope ratios in the central Red Sea (for both water and calcite) [Siddall et al., 2003, 2004]. This relationship was then used to calculate sea level fluctuations from Red Sea oxygen isotope records to within  $\pm 12$  m ( $2\sigma$ ). This uncertainty margin accounts for meteorological variables by taking modern annual maximum and minimum values as the annual average values: a temperature uncertainty is allowed of  $\pm 2^{\circ}\text{C}$ , evaporation uncertainties allow for a range from 1.4 to  $2.8\text{ m a}^{-1}$ , and relative humidity is allowed to vary between 60 and 80%.

[40] This method was developed for planktic foraminiferal records [Siddall et al., 2003, 2004] because the long seawater residence times in the Red Sea at times of low sea levels would cause a long time integration in benthic records. Benthic records would therefore be expected to show a residence-time-based smoothing of any sea level variability, with concomitant artificial reduction in the magnitudes of short-lived events. Siddall et al. [2004] also demonstrated that the central Red Sea is the most suitable region for the technique. In the south, near the sill, the intrusion of a cold layer of Gulf of Aden Intermediate Water during the summer months complicates use of oxygen isotope records. In the north, precipitation originating from the Mediterranean region during the Holocene complicates the interpretation of oxygen isotope records [e.g., Fenton et al., 2000; Arz et al., 2003b].

[41] Recently, Arz et al. [2007] derived a sea level record from benthic oxygen isotopes from the northern Red Sea. These authors used temperature estimates from coccolithophore-based long-chain alkenone unsaturation ratios in order to estimate the sea surface temperature record for their core. They then used this temperature record to remove the temperature component from their down core benthic foraminiferal oxygen isotope record and thus to estimate oxygen isotope changes in the seawater through MIS 3. This oxygen isotope record for water was subsequently empirically scaled to sea level using coral-based sea level estimates. The authors then discussed both the directly measured foraminiferal oxygen isotope record and the inferred seawater oxygen isotope record. By using benthic records, Arz et al. [2007] avoided gaps in their record during aplanktic periods, but, as noted above, benthic

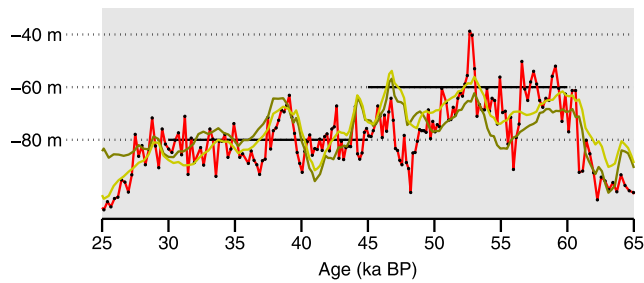


**Figure 8.** A direct comparison of sea level reconstructions from Red Sea oxygen isotopes on an arbitrary common time scale, in this case the time scale of *Siddall et al.* [2003]. Red indicates *Siddall et al.* [2003]. Dark green indicates *Arz et al.* [2007] (temperature corrected). Light green indicates *Arz et al.* [2007] (uncorrected). The ages of *Arz et al.* [2007] are transformed onto the same time scale as those of *Siddall et al.* [2003] by taking tie points at the midpoints of each of the major sea level rises as well as at the MIS 3 to MIS 2 transition (i.e., 24, 39, 47, 53, and 61 ka B.P.).

isotopes in the basin may respond less quickly to varying sea level than the planktic record and may therefore smooth the record of rapid variations in sea level. In addition, the *Arz et al.* [2007] reconstruction was smoothed using a five-point running mean.

[42] Because the underlying sea level forcing is the same for the *Siddall et al.* [2003] and two *Arz et al.* [2007] records, strong similarities should be expected (Figures 7 and 8). Indeed, this expectation is borne out, despite the different locations, the different approaches followed in calibration, and the different chronologies. Figure 8 plots all three records after transformation to a common (arbitrary) age scale in order to better consider the record of sea level variability in the reconstructions (see Figure 8 caption for details of the age scale). All three demonstrate generally higher sea level during early MIS 3 and lower sea level during late MIS 3. All three records include four major sea level fluctuations within MIS 3, with magnitudes between 20 and 30 m.

[43] Removing the temperature signal from the *Arz et al.* [2007] record has very little impact on the resulting sea level reconstruction (Figure 8). This observation corroborates the assumption made by *Siddall et al.* [2003] that temperature effects have little impact on Red Sea oxygen-isotope-derived sea level, which increases confidence in the Red Sea residence time method for sea level reconstruction.

## 2.5. Oxygen Isotope Ratios of Air in Bubbles Trapped in the Vostok Ice Core

[44] *Shackleton* [2000] reexamined the benthic isotope record from equatorial Pacific core V19-30. He assumed an orbitally tuned time scale for both V19-30 and the oxygen isotope ratio of air from bubbles trapped in the Antarctic Vostok ice core. By relying on assumptions about the Dole effect and deep water temperatures, this combination of records allowed him to generate a record of global ice volume/sea level variations. The assumed chronologies for the Vostok ice core records and core V19-30 have a

significant impact on the outcome of this method. *Shackleton's* [2000] revised chronology for the Vostok age scale differs substantially from published age scales, which leads to large disparities in the calculated differences between the ages of ice and trapped (bubbles) gases in the ice core [*Delmotte et al.*, 2004]. Nevertheless, we include the record here for purposes of comparison and completeness (Figure 7).

[45] The *Shackleton* [2000] sea level reconstruction shows some broad similarities with other records included in this paper (Figure 7). It includes four sea level fluctuations of 30–40 m magnitude within MIS 3, and in general, the highest sea levels are recorded at the start of MIS 3.

## 3. DISCONTINUOUS RECORDS

[46] There are many types of discontinuous records of sea level during MIS 3, and we discuss them within three broad classes: (1) fossil corals, the main source of well-dated sea level markers; (2) other markers of (drowned) coastal surfaces; and (3) sediment stratigraphy on continental shelves.

### 3.1. Fossil Coral Reefs

[47] Fossil coral reef data have played a pivotal role in developing our understanding of MIS 3 sea level changes because fossil corals provide material suitable for absolute age dating [*Chappell and Shackleton*, 1986; *Thompson and Goldstein*, 2005, 2006]. This contrasts with down core sediment records, which depend on less reliable techniques such as orbital tuning [*Imbrie et al.*, 1984], comparison to ice core data [*Siddall et al.*, 2003], or comparison to magnetic paleointensity records [*Arz et al.*, 2007]. Certain coral terrace formations such as those on Huon Peninsula in Papua New Guinea in addition provide a stratigraphic framework, with each of the major sea level fluctuations characterized by a distinct terrace that can be dated [*Chappell and Shackleton*, 1986; *Chappell*, 2002]. Further discussion of the evidence for sea level fluctuations from Huon Peninsula is given in section 5.3.

[48] In the absence of a detailed and sequential stratigraphic context (such as that of Huon Peninsula), other uplifted fossil coral reefs yield discontinuous records of sea level change that rely heavily on dating techniques to reveal the actual sequence of sea level events [*Gallup et al.*, 1994; *Stirling et al.*, 1998]. Uncertainty in dating techniques regarding coral samples results in uncertainty in the inferred sea levels because the accuracy of uplift corrections depends on the accuracy of age constraints. Further uncertainties result if reefs are sensitive to the effects of glacioisostatic rebound [e.g., *Lambeck et al.*, 2002]. Section 5.3 offers a detailed comparison of the estimated ages of sea level changes in the coral-based records of *Chappell* [2002] and *Thompson and Goldstein* [2005, 2006].

### 3.2. Other Coastal Features

[49] *Hanebuth et al.* [2006] used Red River delta and Sunda Shelf deposits to make a tentative sea level estimate

for MIS 3 that falls between 60 and 90 m below modern sea level, which compares well with the estimates presented here. To date, there has been little application of this method to sea level variations within MIS 3 on millennial time scales. We note that this technique is likely to be vulnerable to the “broad shelf effect,” when hydroisostatic loading across the shelf due to sea level change has an important impact on the local, relative sea level change [e.g., Bloom, 1967; Johnston, 1993; Milne et al., 1999; Hanebuth et al., 2006]. In addition, this method requires dating that almost invariably relies on the radiocarbon technique which is not very useful for events predating 40 ka. Even for the youngest part of MIS 3, radiocarbon dating carries large uncertainties due to unknown reservoir age corrections and poorly understood calibration between radiocarbon years and calendar years [e.g., Fairbanks et al., 2005; Reimer et al., 2006].

### 3.3. Sediment Stratigraphy

[50] Variations in the sedimentary architecture of the continental shelf and slope have been used to derive sea level records in deeper geological time [Haq et al., 1987; Miller et al., 2005]. The technique is currently being developed for application to MIS 3. Sediment sequences on the shelf/slope of the Gulf of Lions in the Mediterranean demonstrate potential links to sea level fluctuations within MIS 3 [Jouet et al., 2006]. Multiple applications of these techniques, carefully calibrated with datings of the surfaces based on sediment cores, may eventually result in additional control on the record of sea level variability within MIS 3. Uncertainties of this technique relate to the accurate description of sedimentary architecture, the accurate assignment of appropriate depths to that architecture, and accurate corrections for isostatic effects. Isostatic effects may be due to the broad-shelf effect or fluctuations in large ice sheets [Bloom, 1967; Johnston, 1993; Milne et al., 1999].

## 4. COMBINED APPROACHES: SCALED OXYGEN ISOTOPES

[51] Cutler et al. [2003] followed the approach pioneered by Shackleton [1987], in which sea level records are generated through careful scaling of benthic oxygen isotope records using fossil coral data (Figure 7). Cutler et al. [2003] applied rigorous selection criteria to new and previously published U/Th dates to generate a set of coral-based age versus sea level estimates that was subsequently used to provide a sea level scaling for the benthic isotope record of equatorial Pacific core V19-30. This revealed that during glacial periods, the slope of sea level to oxygen isotope variation in core V19-30 is close to  $0.01\text{‰ m}^{-1}$ , as expected for the global mean value [Adkins et al., 2002], while the benthic oxygen isotope values carry an important temperature-related overprint during interglacial periods related to deep ocean warming [Cutler et al., 2003]. Given the similarity of this temperature overprint in both Atlantic and Pacific cores during interglacial periods [Cutler et al., 2003], it would seem that it may well be of a global nature.

No confidence intervals were given for the regression against benthic oxygen isotopes, but the reported confidence intervals for the fossil coral indicators are shown in Figure 7.

[52] Waelbroeck et al. [2002] performed a regression analysis between benthic isotope records and sea level estimates derived from fossil coral data. This regression found that the relation between benthic oxygen isotope values and sea level differed during glacial phases as compared to deglacial phases, likely in response to differences in evolution of deep ocean temperature, hydrography, and other factors influencing the benthic isotope records during these times. The section of their record that is of interest to the present study consists of the Pacific record from core V19-30 prior to 38 ka B.P. and the Atlantic record from core NA87-22 for the interval younger than 38 ka B.P. Because their published sea level reconstruction includes a seven-point running mean that is likely to underestimate any short-term (millennial-scale) variability, we include both the filtered and unfiltered versions of this reconstruction in Figure 7. The uncertainty due to the regression of benthic oxygen isotopes and coral data is larger or equal to  $\pm 13$  m.

[53] The Waelbroeck et al. [2002] record shows three clear fluctuations of around 10–30 m magnitude, with the highest sea levels at the start of MIS 3. The Cutler et al. [2003] record also contains distinct sea level fluctuations, which amount to 30 m or more in magnitude. It shows at least three such millennial-scale sea level fluctuations within MIS 3, but more cannot be excluded given the gaps in the record. Both these analyses find limited temperature effects in the deep Pacific during glacial times but substantial temperature changes between glacial and interglacial periods. This corroborates the previous suggestion by Shackleton [1987] and the inferences made from pore water oxygen isotope values for the last glacial maximum by Adkins et al. [2002] and Adkins and Schrag [2003] that there were only limited temperature effects on benthic oxygen isotope fluctuations in the deep Pacific during glacials, relative to interglacials.

## 5. TIMING AND SYNCHRONIZATION

[54] The discussion about absolute versus relative timing of the MIS 3 sea level variability is marred by many complications and uncertainties. Especially the uncertainty that applies to the absolute timing of Greenland ice core temperature records imposes important limitations on the development of absolute age control for the various sea level records (Figure 9). In the following section and in Figures 9–13 we consider these issues.

### 5.1. Synchronization and Nature of the Benthic Foraminiferal Oxygen Isotope Record

[55] As noted in the introduction, the first independent evidence for the possible phasing between D-O variability and sea level variations during MIS 3 came from core MD95-2042 (3142 m) from the Portuguese margin [Shackleton et al., 2000] (Figure 1). The (surface water)

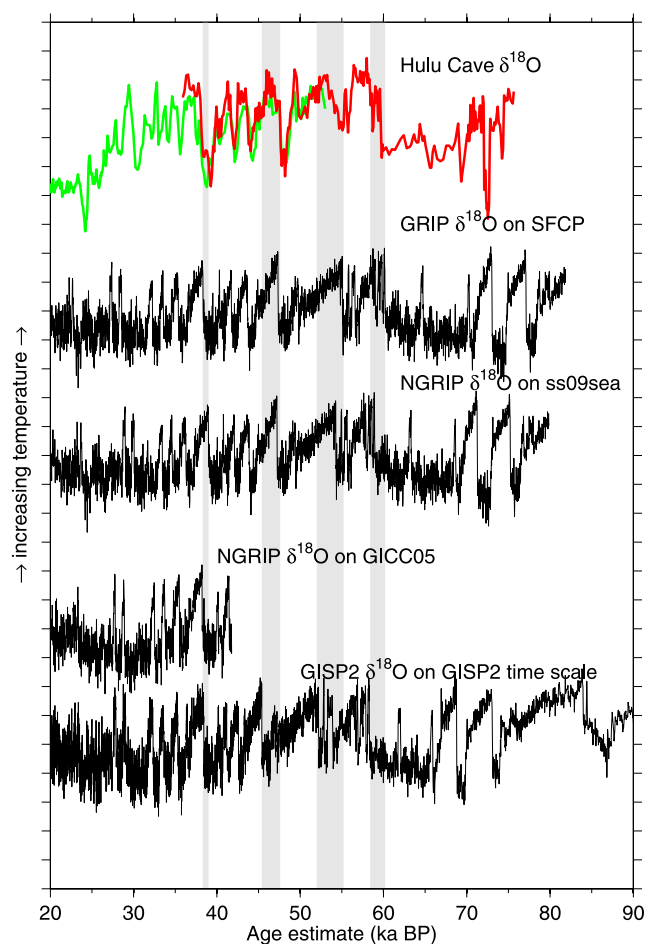


**Figure 9.** A comparison of age scales suggested for MIS 3; see section 5.3 for references. The vertical gray bars indicate the maximum differences between age scales for the major D-O events. There is reasonable agreement between age models for the most recent parts of MIS 3 (~700 years difference), but important disagreements exist of as much as 3000 years for earlier parts of MIS 3 and 2000 years for the onset of MIS 3.

planktic foraminiferal stable oxygen isotope record of this core shows D-O variability that is strongly reminiscent of that found in Greenland ice cores. Coregistered (in the same samples) with this D-O variability in the planktic record, the benthic foraminiferal stable oxygen isotope record displays variability that is remarkably similar to Antarctic climate fluctuations. *Shackleton et al.* [2000] observed that the planktic and benthic records show virtually the same phasing between the two types of variability as the methane-synchronized ice core records from Greenland and Antarctica [*Blunier et al.*, 1998; *Blunier and Brook*, 2001].

[56] Assuming that North Atlantic deep water temperature changes did not affect the timing of MD95-2042 benthic oxygen signal, the MD95-2042 records might simply suggest that the planktic oxygen isotope records reflects Northern Hemisphere climate variability, while the benthic oxygen isotopes reveal the phasing of the sea level variability relative to that Northern Hemisphere climate

record. This indeed was the original interpretation proposed by *Shackleton et al.* [2000, p. 567], who stated,

We suggest that the benthic  $\delta^{18}\text{O}$  record provides evidence of changes in continental ice volume; during stadials when the surface of the North Atlantic was very cold, the surrounding ice sheets were starved of precipitation, and they declined in volume, whereas during the interstadials when the surface was warm, increased precipitation caused these ice sheets to grow. This hypothesis explains the phasing of the benthic  $\delta^{18}\text{O}$  record as well as its character and is also consistent with the observation that the largest amplitude events in the  $\delta^{18}\text{O}$  record are associated with the surface temperature events with the longest duration (in the Greenland record, all events have about the same amplitude but the durations vary).

We note that later studies have confirmed that the magnitudes of Antarctic warming events are proportional to the duration of cold events in Greenland [*Stocker and Johnsen*, 2003; *Siddall et al.*, 2006a; *EPICA Community Members*, 2006]. However, there are indications that changes in benthic oxygen isotope records may have different timings from one ocean to another [*Skinner and Shackleton*, 2005; *Labeyrie et al.*, 2005] and from one depth range to another depth range within the same ocean [*Labeyrie et al.*, 2005; *Waelbroeck et al.*, 2006] because of hydrographic variation between and within ocean basins.

[57] Atlantic benthic oxygen isotope records may be sensitive to past variability in the complicated hydrography of that region. Today, the contrast between the (water) oxygen isotope ratio of pure NADW and pure AABW is of the order of 0.4‰. Note that because NADW is today 2.5°–3.5°C warmer than AABW (equivalent to –0.6 to –0.9‰ in its effect on the isotope composition of calcite), calcite formed in pure NADW will be 0.2–0.5‰ lighter than that formed in pure AABW within the North Atlantic. At the LGM, all bottom water masses may have been close to (surface) freezing temperatures [*Adkins et al.*, 2002; *Adkins and Schrag*, 2003], which would negate any temperature effects associated with water mass switching. Mg/Ca and  $^{13}\text{C}$  data from core MD01-2444K, however, suggest that hydrographic changes and attendant temperature variability may have affected the depth range of NADW during MIS 3 [*Skinner and Elderfield*, 2007; *Skinner et al.*, 2007]. Water mass switching might therefore explain why the oxygen isotope variations in the benthic record of MD95-2042 are larger than expected from variations in sea level of 10–30 m during this period. The question that emerges is “What might be the relative contributions to the benthic oxygen isotope fluctuations during MIS 3 from sea level and hydrographic change”?

[58] Several lines of evidence for sea level change during MIS 3 of 10–30 m magnitude are discussed in this text. This evidence would suggest that the oxygen isotope records of the Portuguese margin cores includes information regarding sea level change that can explain between 50 and 100% of the observed signal, with some superimposed “masking” of that signal by the impacts of hydrographic changes. We note that today (during a well-developed interglacial), the 3146 m deep site of MD95-2042 is considerably influenced by AABW: the site resides just below the transition between NADW and AABW at 3000 m. During glacial times, the water mass transition appears to

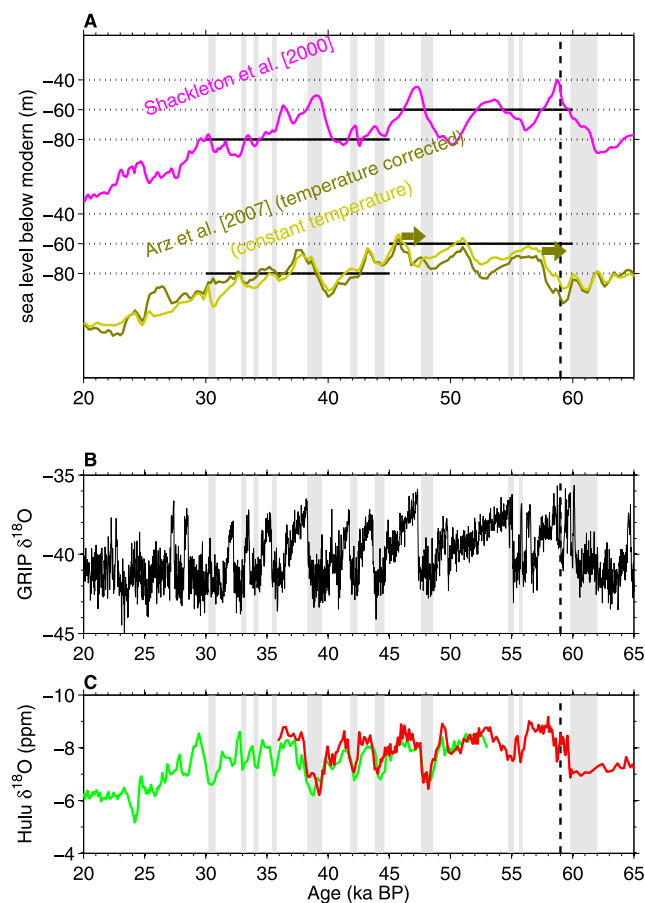


**Figure 10.** (a) Dated records and coral-based records. D-O stadials after Hulu cave  $\delta^{18}\text{O}$  are in gray. Horizontal black lines are at  $-60$  and  $-80$  m and indicate “typical” estimates for the early and late periods of MIS 3, respectively. The sensitivities of the results from the Red Sea method are  $\pm 12$  m (without temperature correction) and  $\pm 8$  m (with temperature correction) [Arz et al., 2007]. Green arrows indicate where there may be an age offset of 2000 years that may explain the age offset between the plots, as discussed in section 5.2. (b) GRIP ice core  $\delta^{18}\text{O}$  on the Shackleton, Fairbanks, Chiu, Parrenin (SFCP) 2004 time scale after Shackleton et al. [2004] (black line). (c) Hulu cave  $\delta^{18}\text{O}$  after Wang et al. [2001]. Grey bars indicate “cold periods” in the Hulu cave record. The vertical black dashed line represents the start of MIS 3 after the Mapping Spectral Variability in Global Climate Project (SPECMAP) estimate.

have resided shallower than today, at 2000–2500 m [Duplessy, 2004; Sarnthein et al., 2003; Curry and Oppo, 2005]. Hence, the benthic oxygen isotope record of MD95-2042 is likely to have been more strongly dominated by AABW at glacial times than today, which would reduce the potential of impacts from any water mass switching.

[59] The discussion presented here makes it very clear that the relationship between temperature, ice volume, and complex hydrographic effects creates complications for the interpretation of benthic oxygen isotope records on the Iberian Margin which will require additional benthic oxygen isotope records, Mg/Ca analyses, and careful efforts to synchronize records. The existing Mg/Ca temperature re-

cord from core MD01-2444K shows fluctuations that do not distort the phasing of the benthic isotope record if the temperature component is removed [Skinner et al., 2007], and so we show the original oxygen isotope here. However, this does not allow for the complications of local hydrography, and so the resulting synchronization can only be taken as a loose indication of the relative timing of sea level fluctuations with respect to temperature fluctuations in the Greenland ice core records.

[60] Pahnke et al. [2003] and Pahnke and Zahn [2005] investigated core MD97-2120 from 1210 m depth in the SW Pacific (a site bathed in lower AAIW) and found a benthic oxygen isotope record with a stratigraphic structure and magnitude variability that is extremely similar to that of NE Atlantic core MD95-2042 (bathed in AABW with possibly some lower NADW). These arguments would imply that a large component of the signal reflects an ice volume/sea level effect, although a considerable overprint of widespread deep-sea temperature fluctuations remains possible, which should be resolved with dedicated proxies.

## 5.2. Synchronization of Sea Level Records From the Red Sea Method

[61] The (relative) chronology of the Red Sea sea level records is another focus of ongoing research. The original Red Sea–based sea level record was assigned a chronology initially on the basis of strong signal similarity with the Antarctic Byrd ice core record and subsequently by correlation to Greenland via the study of Shackleton et al. [2000] [Siddall et al., 2003]. Arz et al. [2007] published a record from the northern Red Sea that was dated using radiocarbon data and by correlation of the magnetic paleointensity record from their core GeoB 5844-2 with the North Atlantic paleointensity stack, which represents a global geomagnetic signal [Laj et al., 2000]. The paleointensity minimum associated with the Laschamp geomagnetic excursion is an important interval recognized in the magnetic paleointensity record of Arz et al. [2007]. This event is expressed in the  $^{10}\text{Be}$  record of Greenland ice cores, within D-O interstadial 10 [Muscheler et al., 2005]; therefore it should offer a sound chronological correlation marker relative to the Greenland climate records because it lies close to a prominent MIS 3 sea level fluctuation [Arz et al., 2007]. This synchronized record is shown in Figure 10.

[62] Overall, Arz et al. [2007] used three paleointensity correlation points to constrain the chronology between 65 and 41 ka. This relatively small number of tie points during this 24-ka interval leads to uncertainties in the synchronization of sea level variability with the Greenland ice cores at millennial-scale resolution, especially if the studied core contains undetected variations in sedimentation rate [cf. Roberts and Winkhofer, 2004]. In addition, uncertainty in the “lock-in” depth of a postdepositional remanent magnetization, which records the paleomagnetic signal, reduces confidence in direct pinning of a sea level event to the Laschamp event [Roberts and Winkhofer, 2004]. The lag involved in the “lock in” of such parameters causes similar

age offsets between the sediment age and the paleointensity signal's age as is seen in ice cores between the ice age and the age of gasses trapped in bubbles within the ice. Because of the lock-in effect, an intensity event will be recorded at a position that is offset downward in the sedimentary sequence relative to its age-equivalent sediment, where the offset reflects the lock-in depth. Lock-in depths typically range between about 5 and 15 cm [Roberts and Winkhofer, 2004]. Hence, the use of magnetic paleointensity events to synchronize the Red Sea sea level record to Greenland ice core records may result in a systematic offset toward younger ages relative to Greenland, by an amount equivalent to the age equivalent of the lock-in depth. In the northern Red Sea core, with an accumulation rate of  $7.5 \text{ cm ka}^{-1}$ , this offset could amount to 650–2000 years (using a lock-in depth between about 5 and 15 cm). Age offsets of 2000 years may explain the difference between the timing of the Shackleton et al. [2000] and Arz et al. [2007] records (Figure 10). We refer to Rohling et al. [2008] for a more complete review of this topic.

[63] Further advances in establishing the temporal relationship between the Red Sea sea level records and the D-O and AA-style climate rhythms may be expected from detailed multiproxy investigation of Red Sea sediment cores to distinguish coregistered records, within one set of samples, of planktic foraminiferal stable oxygen isotope (sea level) variations and local environmental variability. The testable hypothesis would be that the latter, especially windblown dust flux data, will reveal a distinct D-O-style signal, since this is the predominant rhythm of climate variability in the Indian/Asian monsoon region [Schulz et al., 1998; Sirocko, 2003; Burns et al., 2003; Wang et al., 2001]. Such a multiproxy study would, therefore, result in unambiguous, coregistered recording of the phase relationship between the D-O-style fluctuations and the sea level record. Recently, Rohling et al. [2008] carried out such a study and found that windblown dust flux data supported the notion that global sea level varied on an AA-style climate rhythm during MIS 3.

### 5.3. Absolute Timing

[64] Determining the absolute timing of D-O events remains a challenge. There are several Greenland ice core time scales, based primarily on layer counting and/or glacial modeling [e.g., Johnsen et al., 1995, 2001; Meese et al., 1997; Shackleton et al., 2004; Rasmussen et al., 2006; Andersen et al., 2006; Svensson et al., 2006] (Figure 9). Here we discuss these age models in the context of MIS 3. The Shackleton, Fairbanks, Chiu, Parrenin (SFCP) 2004 time scale (during MIS 3) is synchronized to the Hulu Cave record at the start of MIS 3 and to the ss09sea time scale [Johnsen et al., 2001] for Greenland ice cores [Shackleton et al., 2004] at the end of MIS 3. Shackleton et al. [2004] note that offsets of several hundred years remain between the Hulu Cave and ss09sea time scales during the early part of MIS 3.

[65] Given that the chronologies of the various Greenland ice cores are continuously being improved, no time scale

can yet be taken as definitive. Although we proceed with comparisons between sea level reconstructions and ice core records on the Hulu/SFCP time scale, it is interesting to note that the new multiproxy layer-counted GICC05 time scale (reaching 40 ka) for the Dye3, Greenland Ice Core Project (GRIP), and North Greenland Ice Core Project ice cores [Rasmussen et al., 2006; Vinther et al., 2006] shows reasonable agreement with the Greenland Ice Sheet Project 2 (GISP2) time scale that was also layer counted down to at least 40 ka [Meese et al., 1997]. These time scales have been compared in detail by Andersen et al. [2006] and Svensson et al. [2006]. Here we show the high-resolution GISP2 record of Stuiver and Grootes [2000]. We note that the SFCP time scale [Shackleton et al., 2004] shows considerably bigger offsets from the GISP2 time scale for the period 40–80 ka. The SFCP time scale was developed for the GRIP ice core record [Shackleton et al., 2004], and so we will refer to the GRIP ice core record in Figures 10–13. We encourage readers to refer back to Figure 9 for an illustration of the overall uncertainties in the absolute dating of MIS 3 climate variability.

[66] How have absolute dates been placed on sea level fluctuations during MIS 3? Huon Peninsula in Papua New Guinea consists of an uplifted set of terraces that records past sea level fluctuations. Importantly, the section of the coastal zone corresponding to MIS 3 comprises several such terraces, which likely formed as a result of sea level variations within MIS 3. Chappell [2002] used a combination of U/Th dated (alpha counting and thermal ionization mass spectrometer) coral terraces, river sediment deposits, and a simple model of coral terrace formation on an uplifting coast to derive a sea level curve for Huon Peninsula through MIS 3. This comprehensive approach combines a detailed stratigraphic understanding of the entire Huon terrace formation and careful dating controls to develop an in-depth understanding of the record of sea level fluctuations. As a consequence, the record contains more information on the timing and nature of sea level fluctuations than just the relatively small number of dated fossil corals. Figure 11 includes the sea level record from the stratigraphic modeling of Huon terraces by Chappell [2002], which is representative of the other Huon Peninsula studies [Yokoyama et al., 2001; Esat and Yokoyama, 2006]. Chappell [2002] concluded that sea level rises coincided with major cold D-O stadials in the Greenland records (specifically with Heinrich events), on the basis of a comparison between U/Th ages and the GISP2 time scale. Subsequent work supported this conclusion [Esat and Yokoyama, 2002, 2006].

[67] Without careful screening a reliable sea level record cannot be derived from coral reef data [e.g., Gallup et al., 1994; Cutler et al., 2003], but screened or corrected records provide increasingly reproducible results. Indeed, many studies of fossil corals point out that many potential dating points need to be rejected, since they fail to meet the required criteria for closed system behavior [e.g., Stirling et al., 1998]. This requirement has thus far inhibited the development of an independent, highly resolved, sea level

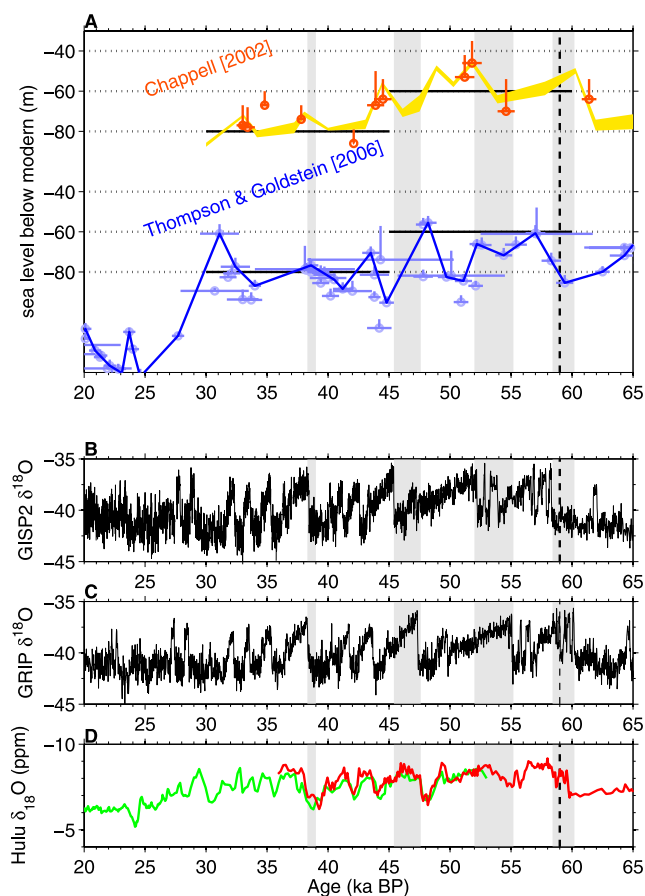


**Figure 11.** (a) Dated records and coral-based records. Horizontal black lines are at  $-60$  and  $-80$  m and indicate “typical” estimates for the early and late periods of MIS 3, respectively. Errors in the fossil reef based techniques are shown on the plot. (b) Greenland Ice Sheet Project 2 (GISP2) ice core  $\delta^{18}\text{O}$  [Grootes and Stuiver, 1997]. (c) GRIP ice core  $\delta^{18}\text{O}$  on the SFCP time scale after Shackleton *et al.* [2004] (black line). (d) Hulu cave  $\delta^{18}\text{O}$  after Wang *et al.* [2001]. Grey bars indicate the uncertainty in the timing of the major stadal-interstadial transitions as in Figure 6. The vertical black dashed line represents the start of MIS 3 after the SPECMAP estimate.

record based on coral samples [Cutler *et al.*, 2003]. Thompson and Goldstein [2005, 2006] applied a new method to correct U/Th dated corals for open system behavior, resulting in a large increase in the number of fossil-reef-based sea level estimates. As in all multiregional compilations, care is due when interpreting the Thompson and Goldstein [2005, 2006] record where it comprises data from different sites with different uplift rates. However, all coral indicators used in the MIS 3 section of their sea level record originate from Huon Peninsula and are therefore internally consistent. Unlike the reconstruction of Chappell [2002], the work of Thompson and Goldstein [2005, 2006] takes only limited account of the stratigraphic context within which corals were recovered.

[68] The fossil coral data and reconstructed sea level records of Thompson and Goldstein [2005, 2006] and Chappell [2002] are compared in Figure 11. Both recon-

structions show generally higher sea level in the earlier part of MIS 3 than toward the end, and both show at least four sea level fluctuations of 20–30 m magnitude. In the context of absolute timing we note that the Thompson and Goldstein [2005, 2006] age estimates offer close matches to the orbital SPECMAP timing of stadal to interstadial transitions of the last three glacial cycles.

[69] Despite the similarities between the records there are important differences between the Chappell [2002] and Thompson and Goldstein [2005, 2006] sea level estimates, and we discuss these here. The open system correction carried out by Thompson and Goldstein [2005] makes most of the Huon ages older and the uplift-corrected sea levels therefore lower. It is the shift to older and lower data points, as well as the addition of data from Cutler *et al.* [2003], that changes the timing of the MIS 4–3 transition between the reconstructions of Chappell [2002] and Thompson and Goldstein [2005, 2006]. The ages in the Chappell [2002] paper were first published by Chappell *et al.* [1996] and are not strictly closed system ages: the initial  $\delta^{234}\text{U}$  ranges from 132 to 144 while the modern seawater value is  $\sim 145$ –146, which brings into question the reliability of these ages. Because many of the original ages were alpha counted the precision on the measured  $^{234}\text{U}/^{238}\text{U}$  was insufficient for this ratio to be useful as a screening tool or a correction constraint. Alpha-counted ages, ages with  $\delta^{234}\text{U}$  of poor precision, and corals with significant calcite were excluded from the Thompson and Goldstein [2005, 2006] analysis. Of the 12 data points supporting the Chappell [2002] curve, 7 were alpha counted, and these were therefore rejected for the Thompson and Goldstein [2005, 2006] analysis. Of the five corals remaining, only two act as defining points on the Thompson and Goldstein [2005, 2006] record. The Thompson and Goldstein [2005, 2006] curve contains additional high-precision Huon data from Cutler *et al.* [2003]. For these reasons, it is not surprising that the two sea level curves are different in detail. Rather, it is encouraging that they retain a lot of structural similarity, given that they have so few data points in common.

#### 5.4. Synthesis

[70] Here we compare in detail the phasing of sea level change for both the synchronized and dated records that were discussed. We look in detail at the sea level shifts at around 40–38 ka B.P. and around the MIS 4–3 transition (Figures 12 and 13).

[71] Differences between the various reconstructions are partly due to ambiguity in the choice of curve drawn through the discrete fossil coral points of Thompson and Goldstein [2005]. As noted by those authors, the curve drawn through the data is not unique. This is clearer if we look at detailed plots of specific sea level fluctuations (Figures 12 and 13). In most instances, discrete data points remain in fairly good agreement with the Arz *et al.* [2007] and Chappell [2002] sea level estimates. The Thompson and Goldstein [2005, 2006] curve seems to agree with the Arz *et al.* [2007] sea level reconstruction at the start of MIS 3 (Figure 13), but there are some differences between these



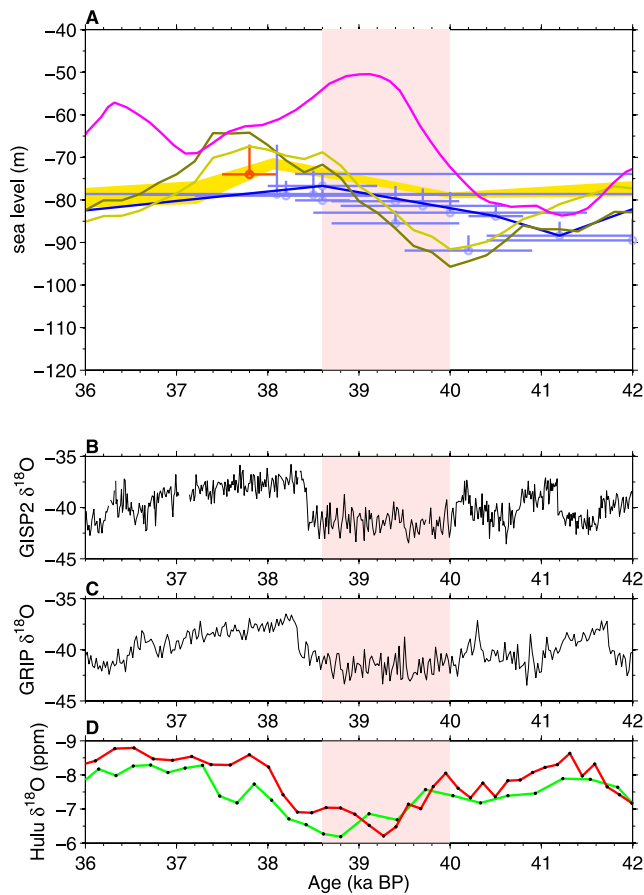


**Figure 12.** (a) Dated records and coral-based records. Colored lines are the same as in Figures 10 and 11: *Chappell* [2002] (yellow with orange crosses), *Thompson and Goldstein* [2005] (dark blue with light blue crosses), *Arz et al.* [2007] with temperature corrected (dark green) and without temperature correction (light green), and *Shackleton et al.* [2000] scaled after the method described in section 2.1 (pink). Errors in the fossil reef based techniques are shown on the plot. The sensitivities of the results from the Red Sea method are  $\pm 12$  m (without temperature correction) and  $\pm 8$  m (with temperature correction) [*Arz et al.*, 2007]. (b) GISP2 ice core  $\delta^{18}\text{O}$ . (c) GRIP ice core  $\delta^{18}\text{O}$  on the SFCP time scale after *Shackleton et al.* [2004] (black line). (d) Hulu cave  $\delta^{18}\text{O}$  after *Wang et al.* [2001] for two different speleothem records (red and green). The period of sea level increase is in pink.

same records during later periods (compare Figures 10 and 11). The analysis presented in this section will consider the timing of the changes and not the absolute value of the sea level positions.

[72] Figure 12 shows the four attempts at defining the ages of the MIS 3 sea level fluctuations [*Chappell*, 2002; *Thompson and Goldstein*, 2005; *Arz et al.*, 2007; *Shackleton et al.*, 2000], and our interpretation of the results of *Shackleton* [2000] (see Figure 3) are shown for the sea level transition at around 39 ka B.P. Given the challenges in creating the various sea level records, there is remarkable agreement in the timing of the sea level rise over this period. This timing clearly places the sea level rise during a period

in the Hulu Cave record linked to a cold phase in Northern Hemisphere climate and a warming phase in Antarctica (i.e., Southern Hemisphere).

[73] Additional information is available from a strong freshening in the Gulf of Mexico during this period, which has been linked to melting of the Laurentide ice sheet [*Hill et al.*, 2006]. This record has been tied to the SFCP time scale using the coincidence of the Laschamp event in the Gulf of Mexico and GRIP records. Such a synchronization

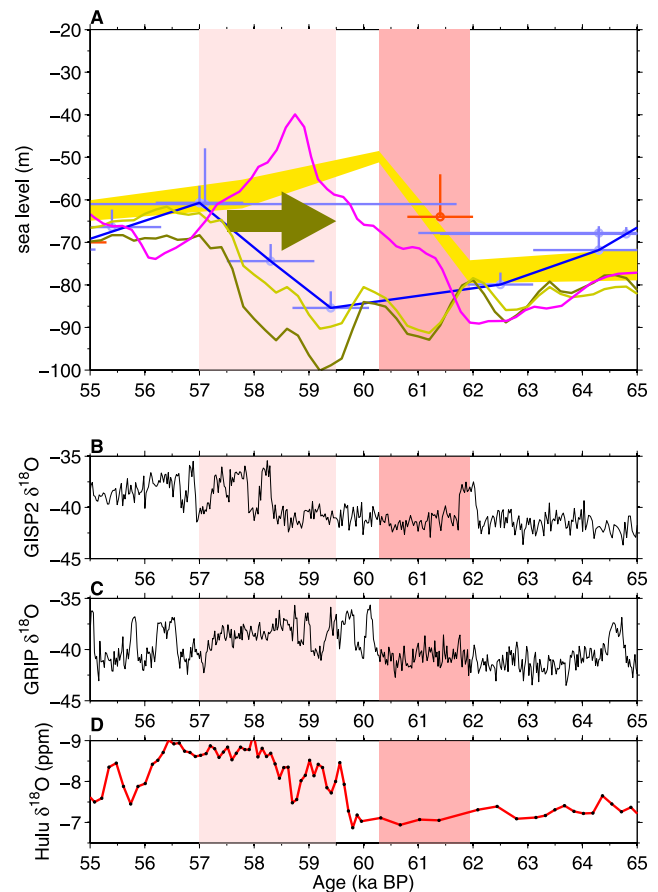


**Figure 13.** (a) Synchronized records and coral-based records. Colored lines are the same as in Figure 4: *Chappell* [2002] (yellow with orange crosses), *Thompson and Goldstein* [2005] (dark blue with light blue crosses), *Arz et al.* [2007] with temperature corrected (dark green) and without temperature correction (light green), and *Shackleton et al.* [2000] scaled after the method described in section 2.1 (pink). Errors in the fossil reef based techniques are shown on the plot. The sensitivities of the results from the Red Sea method are  $\pm 12$  m (without temperature correction) and  $\pm 8$  m (with temperature correction) [*Arz et al.*, 2007]. (b) GISP2 ice core  $\delta^{18}\text{O}$ . (c) GRIP ice core  $\delta^{18}\text{O}$  on the SFCP time scale after *Shackleton et al.* [2004] (black line). (d) Hulu cave  $\delta^{18}\text{O}$  after *Wang et al.* [2001]. The period of sea level increase in the *Arz et al.* [2007] and *Thompson and Goldstein* [2005] records is in lighter pink. The period of sea level increase in the *Chappell* [2002] record is in darker pink. The green arrow indicates where there may be an age offset of 2000 years that may explain the age offset between the plots, as discussed in section 5.2.

and the best information available from dated sea level records reveals that the Laurentide ice sheet apparently provided a considerable freshwater flux into the Gulf of Mexico during the D-O stadial and that the surface freshening signal in the Gulf of Mexico persisted into the subsequent D-O interstadial.

[74] Regarding the timing of the MIS 4–3 transition, all the reconstructions are in reasonable agreement with the SPECMAP estimate of 59 ka B.P. (Figures 10 and 11). However, the records differ in detail (Figure 13). For the curves of *Thompson and Goldstein* [2005, 2006] and *Arz et al.* [2007], the transition occurs during a phase in the Hulu cave record which is linked to a warm phase in Greenland. The *Chappell* [2002] curve and our interpretation of *Shackleton et al.* [2000] differ from the other two approaches in that they suggest an earlier age for the start of MIS 3, in line with increases in Antarctic temperature and a relatively cold period in Greenland.

[75] There remain significant uncertainties about the absolute age constraints of the dominant Northern Hemisphere climatic fluctuations and about the dating/synchronization techniques used to constrain sea level changes during MIS 3. The *Arz et al.* [2007] and *Thompson and Goldstein* [2005, 2006] reconstructions do not reveal a consistently reproducible picture of the timing of sea level change with respect to large-scale changes in climate through the duration of MIS 3. An age offset of up to 2000 years might explain this discrepancy for the *Arz et al.* [2007] record (see section 5.2), and we also reiterate the fact that there remain considerable uncertainties about the absolute chronologies of the various ice core records.

[76] Sea level may not have followed systematic, repeating patterns during MIS 3, which one might link in a consistent fashion with similar records of temperature change. However, an impressive number of different records capture the Greenland and Antarctic climate events and the systematic, repeating patterns of their variation during MIS 3. It seems unlikely that global ice volume acted independently of large-scale temperature changes during MIS 3. We therefore propose that a good test of dating/synchronization techniques for temperature and sea level records through MIS 3 is that they give mutually consistent, repeated patterns, similar to the synchronized temperature records of Antarctica and Greenland [*Blunier and Brook*, 2001; *EPICA Community Members*, 2006]. Note that the lagged response of ice sheet growth to temperature change suggests that the ice volume response may be more complicated than the response of Antarctic temperature to D-O events.

### 5.5. Ice Sheet Growth Rates

[77] Despite the difficulties related to intercomparison of records on “absolute” time scales, other information can be obtained from the various sea level records we present in this paper. The growth rates of the large continental ice sheets may be estimated even from records that lack absolute time scales or are discontinuous. For example *Cutler et al.* [2003] used two Huon Peninsula corals to

estimate ice sheet growth rates of 1–2 cm a<sup>-1</sup> (sea level equivalent units are used throughout the paper) for the MIS 5–4 transition and used the benthic oxygen isotope record of core V19-30 to imply that similar growth rates occurred during MIS 3. Dependence on any one site for a “typical rate of ice sheet growth” leaves the possibility of bias due to local isostasy. It is therefore very significant that this result is replicated during other periods, at other sites, and using alternative methods. *Siddall et al.* [2003] found growth rates of the order of 2 cm a<sup>-1</sup> on the basis of their reconstructions from a central Red Sea planktic oxygen isotope record [see also *Rohling et al.*, 2004], a value that was corroborated by work on the northern Red Sea [*Arz et al.*, 2007]. U/Th dated coral estimates that were corrected for open system effects [*Thompson and Goldstein*, 2005, 2006] also support ice sheet growth rates during MIS 3 of 1–2 cm a<sup>-1</sup>, and this rate is found at multiple sites by these authors. There are additional periods in the sea level history that illustrate similar growth rates, and these will be further described in section 6.3 below.

## 6. INTERPRETATION AND DISCUSSION

### 6.1. Synthesis of MIS 3 Sea Level Reconstructions

[78] Although some ambiguities remain between the various records, we find that a common millennial-scale stratigraphy emerges from the studies of MIS 3 sea level considered here. The stratigraphic characteristics of all of the reconstructions are summarized in Table 1. All the dated curves are in reasonable agreement with the SPECMAP estimate for the MIS 4–3 transition of 59 ka B.P. [*Imbrie et al.*, 1984]. It is tempting to suggest that insolation drove sea levels to be ~20 m higher during the first half of MIS 3 compared to the latter half, although the relationship between insolation and ice volume is likely to be complicated during the glacial period [e.g., *Huybers*, 2006]. An alternative explanation will be given in section 6.5. Superimposed on this longer-term change are at least four millennial-scale sea level fluctuations of 20–30 m magnitude. This estimate relies principally on the Red Sea isotope records and the fossil coral data but is strongly supported by other indicators such as the benthic oxygen isotope records. The presence of four major fluctuations does not rule out higher-frequency, lower-magnitude variations during MIS 3 that are not resolved by the techniques included here but which might be feasible given a potential ice sheet growth rate of 1–2 cm a<sup>-1</sup>. New, highly resolved records from a variety of techniques are needed to assess whether such higher-frequency events may have existed.

[79] A stratigraphy of four sea level fluctuations during MIS 3 does not close the debate on the timing of sea level change; both Antarctic (Southern Hemisphere) timing or Greenland (Northern Hemisphere) timing are equally plausible. For example it could be argued that ice volume is the result of ice sheet growth/reduction integrated over the cold/warm intervals linked to the sequence of four Bond cycles during MIS 3. Alternatively, one may argue that the presence of four fluctuations links changes in global ice

volume with the timing of Antarctic (Southern Hemisphere) warm events A4–A1 [e.g., *Siddall et al.*, 2003; *Rohling et al.*, 2004]. Indeed, *Clark et al.* [2007] argued that Bond cycles, Antarctic (Southern Hemisphere) warm events, and sea level changes are all linked. As discussed in this text, there is growing evidence to help decide this question.

[80] In Figures 12 and 13, we have considered in detail two well-defined sea level transitions using four different approaches giving a total of eight records of instances of rapid sea level change. In six out of those eight records the rapid sea level change would appear to coincide with a period in the Hulu cave record that relates to a cold phase in Greenland and warming phase in Antarctica. For the sea level rise at around 39 ka B.P., all four records indicate rising sea level during a cold period in Greenland (Figure 12). This is supported by indications of strong freshening of the Gulf of Mexico during the same event [*Hill et al.*, 2006], which would suggest that fluctuations in the volume of the Laurentide ice sheet are at least partly responsible for the most recent of the large MIS 3 ice volume fluctuations (this does not suggest that the Laurentide contribution excludes any contribution from Antarctica, as suggested by *Rohling et al.* [2004]). With the improvements to techniques and time frames, a convergence seems to be emerging of available evidence on rises in sea level during the cold phases in Greenland and warming phases in Antarctica. The agreement between techniques is stronger for more recent events, which may be due to the decrease in the uncertainties of age models with more recent periods (Figures 12 and 13).

## 6.2. Ice Sheet Response/Feedback

[81] It is commonly assumed that ice sheet growth over a glacial cycle follows a sawtooth pattern of very slow ice sheet growth during the glacial period and rapid loss during the glacial termination [see, e.g., *Imbrie et al.*, 1984; *Bintanja et al.*, 2002; *Huybers and Wunsch*, 2004; *Lisiecki and Raymo*, 2005]. However, this assumption is challenged by observations of rapid changes in eustatic sea level from coral indicators which indicate rapid increases in ice volume during several important transition periods: the MIS 5–4 transition [*Cutler et al.*, 2003], the MIS 5e–5d transition [*Andrews and Mahaffy*, 1976; *Lambeck et al.*, 2002], and during a reversal within the sea level rise of the penultimate deglaciation [*Esat et al.*, 1999; *Siddall et al.*, 2006b; *Thompson and Goldstein*, 2005, 2006]. Recently reported data from Barbados also support the possibility of rapid ice sheet growth during the MIS 3–2 transition [*Lambeck et al.*, 2002; *Peltier and Fairbanks*, 2006]. All of these studies indicate values between 1 and 2 cm of sea level equivalent ice sheet growth per year, which would agree with the estimates for MIS 3 derived here.

[82] Many ice sheet models are forced, at least in part, using reconstructions of Greenland temperature [see, e.g., *Marshall and Clarke*, 1999; *Bintanja et al.*, 2002; *Arz et al.*, 2007]. This approach assumes that temperature over the major Northern Hemisphere ice sheets followed similar trends to temperatures inferred from the Greenland

ice core records. This assumption obviously does not hold during interglacial periods, when the Laurentide ice sheet is not present (and therefore does not vary in line with Greenland temperature); one may then ask when the transition is between the glacial phase (when Greenland temperature variations may be linked to changes in the Laurentide ice sheet) and the interglacial phase (when there is no Laurentide ice sheet). Modeling attempts forced with the Greenland temperature fluctuations have struggled to generate ice sheet growth rates that could match the observational estimates of ice sheet growth during the key phases of the last glacial cycle [see, e.g., *Marshall and Clarke*, 1999; *Bintanja et al.*, 2002]. This questions the suitability of the seemingly straightforward assumption that the large Northern Hemisphere ice sheets waxed and waned in response to the climate rhythm expressed by the Greenland (D-O) temperature fluctuations [*Marshall and Clarke*, 1999].

[83] *Denton et al.* [2005] suggest that variability of the Laurentide Ice Sheet (LIS) may have been dominated by summer melting and so would not have been directly influenced by the (winter-dominated) temperatures recorded by the Greenland ice core proxy data. In support of this analysis, *Hill et al.* [2006, p. 8] conclude their analysis of the phasing of meltwater input into the Gulf of Mexico stating that “. . . our results indicate that growth/decay fluctuations of the LIS may have been decoupled from Greenland air temperature history during MIS 3.” The present study supports the argument of *Denton et al.* [2005] by postulating a distinction between the temperature variations recorded in the Greenland ice core temperature proxy records and the mechanisms that control the waxing and waning of the major ice sheets. Recently, *Schaefer et al.* [2006] compiled evidence for the retreat of many mountain glaciers worldwide during the last termination. They suggest that the initiation of the retreat of these mountain glaciers would appear to be synchronous with the commencement of warming in Antarctica.

[84] Temperatures across much of the Northern Hemisphere are thought to be strongly influenced by ocean heat transport in the Atlantic [e.g., *Rahmstorf*, 2002; *Stocker and Johnsen*, 2003; *EPICA Community Members*, 2006]. The transport of heat in the North Atlantic is generally attributed to variations in the region’s surface buoyancy (which controls the convection of surface waters to the deep ocean), which in turn is influenced by Heinrich events and meltwater influxes from the Northern Hemisphere ice sheets [e.g., *Ganopolski and Rahmstorf*, 2001; *Knutti et al.*, 2004]. However, oceanic responses do not seem to be straightforward with respect to either the rate or magnitude of meltwater fluxes and vary between different observational techniques, models, and hypothetical scenarios [*Rohling et al.*, 2004; *Roche et al.*, 2004; *Stanford et al.*, 2006]. Such linked processes necessitate coupled modeling, rather than stand-alone models of ice sheet growth or ocean responses to meltwater input, in order to develop an understanding of the phasing between ice volume variations and the temper-

ature records of Antarctica and Greenland. Such efforts are discussed in sections 6.3 and 6.4.

### 6.3. Climate Modeling

[85] *Stocker and Johnsen* [2003] considered a conceptual model of the thermal bipolar seesaw to address climatic variability during MIS 3. In their model the temporal behavior of temperature at high southern latitudes is not in strict antiphase to that in high northern latitudes, but instead it represents an integration in time due to thermal storage in the Southern Ocean. Essentially along the axis of the Atlantic, the temperature change responds as a seesaw. If the AMOC should collapse during a period of freshwater input into the North Atlantic, then reduced oceanic heat flux toward the North Atlantic would drive a decrease in temperature in the North Atlantic. Reduced oceanic heat flux to the North Atlantic is linked to heat retention in the south, which then drives an increase in temperature in the South Atlantic. Heat transfer along the length of the Atlantic is suggested to be efficient because of transfer of energy via Kelvin waves along the margins. The transfer of heat across the Southern Ocean is less efficient and is dominated by horizontal mixing by eddies [e.g., *Keeling and Visbeck*, 2005]. Heat takes time to cross the Southern Ocean in this way and therefore the increase in Antarctic temperatures lags the South Atlantic signal. In fact, the Antarctic signal is suggested to be “catching up” with the North Atlantic forcing during D-O stadials, so that Antarctica continues to warm as long as the D-O stadial persists; Antarctic warming/cooling would therefore be proportional to the duration of the D-O stadial/interstadial periods [*Stocker and Johnsen*, 2003].

[86] Although this model would explain much of the variance observed, the simple thermal bipolar seesaw is not entirely satisfactory because the time scale needed to characterize the heat transfer across the Southern Ocean was found to be considerably longer than that suggested by dynamical models [*Stocker and Johnsen*, 2003]. This inconsistency was addressed using a three-dimensional ocean circulation model coupled to a simple atmosphere model [*Knutti et al.*, 2004]. These authors simulated meltwater input in the North Atlantic by reducing surface salinity there (i.e., by removing salt). The removal of salt in the North Atlantic was compensated by the addition of salt to the ocean surface elsewhere. Such removal of buoyancy from the ocean surface in much of the ocean may bias the results, which nevertheless remain interesting to consider. The model suggests that meltwater injections into the North Atlantic affected Atlantic circulation in two ways. First, the mechanism of reducing or halting the production of North Atlantic Deep Water appears important, in agreement with *Stocker and Johnsen* [2003]. Second, the meltwater input was found to also have a direct effect on Atlantic circulation by displacing isopycnal surfaces, which ultimately slowed down the Antarctic response in addition to the effect of Southern Ocean mixing time scales. *Knutti et al.* [2004] provided a simple, conceptual model of this effect, which linked the Antarctic response to the duration of the cold D-O

stadial (as *Stocker and Johnsen* [2003]) but also to the magnitude of the meltwater pulse. This model implies that freshwater input occurred largely during Greenland cold phases. According to the model, freshwater input may also impinge on Greenland warm phases if a threshold value of the freshwater input is not crossed. Integration of the modeled freshwater forcing would imply that the ice sheet reduction occurred during Greenland stadials, and ice sheet increase occurred during Greenland interstadials. Essentially, this argues for an Antarctic-style timing of ice volume/sea level fluctuations, as was suggested by the benthic oxygen isotope record of *Shackleton et al.* [2000] and the original Red Sea sea level study of *Siddall et al.* [2003; see also *Rohling et al.*, 2004]. *Knutti et al.* [2004] focused on the climatic response to freshwater input in the North Atlantic and therefore do not provide an explanation as to why the ice sheets might behave in this way. The absolute values of the changes in ice sheet volume during this period as implied by *Knutti et al.* [2004] are model-dependent and sensitive to the model set up and are therefore not reported in their paper.

### 6.4. Coupled Ice Sheet and Climate Modeling

[87] Several conceptual and numerical models have attempted to consider the coupled response of ice sheet and temperature fluctuations from different perspectives. Here we consider a few of these models.

[88] *Clark et al.* [1999] suggested that at intermediate stages of the growth of the Laurentide ice sheet (i.e., for periods similar to MIS 3), there could be a self-sustained cycle related to the position of the southern edge of the ice sheet relative to a threshold latitude. At this latitude, meltwater is restricted to flow southward via the Mississippi, and above this latitude, meltwater flows northward into the polar North Atlantic. It was suggested that if the southern edge of the Laurentide ice sheet receded to the north of the threshold latitude, then meltwater would flow into the polar Atlantic, reducing the AMOC and the heat transport to the North Atlantic. The reduced poleward heat transport would then cool the region of the Laurentide ice sheet and promote a positive mass balance. With positive mass balance the ice sheet would grow, and the southern edge of the ice sheet would migrate southward. Once south of the threshold latitude, meltwater would be diverted into the Caribbean via the Mississippi and would no longer restrict the AMOC. With a reinvigorated AMOC, poleward heat transport would increase, raising the temperature in the region of the Laurentide ice sheet and creating a negative mass balance. Negative mass balance causes a reduction in the ice sheet and a northward migration of the southern edge of the ice sheet so that the cycle starts again. Conceptual models such as that proposed by *Clark et al.* [1999] need careful validation with more quantitative, dynamic models such as that described in the next paragraph.

[89] Simulations of ice sheet variability during MIS 3 with the coupled low-resolution Climate and Biosphere Model (CLIMBER) Earth system model [e.g., *Arz et al.*, 2007] contrast with the results of *Knutti et al.* [2004]. The

CLIMBER simulations suggest ice sheet growth during Greenland D-O stadials, when increased moisture transport to the region of the Laurentide ice sheet and reduced temperatures would support the growth of ice sheets. Conversely, the model suggests ice sheet reduction (sea level rise) during the warm D-O interstadials.

[90] A recent study by *Clark et al.* [2007] applies the atmospheric moisture transport fields from an atmospheric general circulation model to a mass balance model of the Northern Hemisphere ice sheets. As an extension of the seesaw concept, these authors put forward the notion that temperature in the equatorial Pacific may be linked to Antarctic temperatures via water masses that are subducted in the Southern Ocean and upwelled in the equatorial Pacific. Using this reasoning, an atmospheric climate model is driven by both a hypothetical temperature variation in the equatorial Pacific, which follows the Antarctic temperature reconstructions, and the Greenland temperature reconstructions. The moisture transport from this model was in turn used to drive a mass balance model of the major Northern Hemisphere ice sheets. The results from this modeling work suggest that the growth of the major Northern Hemisphere ice sheets was linked to temperature changes in the North Atlantic as well as the equatorial Pacific, which in turn are linked to changes in Antarctic temperature. The resulting waxing and waning of the ice sheet then follows a pattern with a timing similar to that of Antarctic temperature variability, with decreases in ice volume (increases in eustatic sea level) during cold periods in the Greenland temperature records. In agreement with data summarized here, the model simulations resulted in four sea level fluctuations of 10–20 m magnitude. This model presents a possible mechanism for an internal oscillation in the ice-ocean-atmosphere system on time scales set by ocean mixing and the ice sheet response.

[91] It is obvious that both data and modeling can be (and have been) used to make either phasing argument for the sea level variability. The solution to this conundrum will require new, highly resolved, coregistered data of sea level fluctuations and regional (either D-O-style or Antarctic-style) climate variability and fully coupled models (ice-ocean-atmosphere) with complete representation of ice sheet dynamics that can be run in transient modes.

### 6.5. A Conceptual “Limiting Ice Sheet Growth/Loss Model”

[92] Given the discussion in section 6.2 about the apparent maximum sustainable rates of ice sheet growth of 1–2 cm a<sup>-1</sup>, we now develop a simple model of ice sheet growth and decay based on two simple assumptions: (1) Ice sheet growth is rate limited to 1 cm a<sup>-1</sup> and (2) ice sheet loss is constrained to a similar rate. We base assumption 1 on the reconstructed rates of ice sheet growth from the literature [*Esat et al.*, 1999; *Cutler et al.*, 2003; *Siddall et al.*, 2003, 2006b; *Thompson and Goldstein*, 2005, 2006] and recent modeling efforts that have managed to reconstruct ice sheet growth rates of this magnitude [*Peltier and Fairbanks*, 2006] (see section 6.2). Assumption 2 is based

on the near symmetry of the rises and falls in sea level during MIS 3 that is apparent in all of the sea level reconstructions presented in this paper. In summary, ice volume is either allowed to increase or decrease at a fixed rate of 1 cm a<sup>-1</sup> depending on whether it is a cold or warm period in Greenland. Note that assumption 2 is based on observational constraints of sea level variation during MIS 3. During the termination of the last glacial period the maximum rate of ice sheet reduction reached 3–5 cm a<sup>-1</sup>, as constrained by both Barbados [*Fairbanks*, 1989; *Stanford et al.*, 2006] and Tahiti corals [*Bard et al.*, 1996], greater than the maximum observed rates of ice sheet growth during the glacial period of 1–2 cm a<sup>-1</sup>. Although the termination of the last glacial period is not necessarily analogous to MIS 3, we include sensitivity tests to illustrate the effect of increased rates of ice sheet reduction compared to ice sheet growth.

[93] We first represent the growth and decay of global ice volume by increasing/decreasing global ice volume during Greenland cold/warm intervals on the GRIP SS09 time scale [*Johnsen et al.*, 2001; *Blunier and Brook*, 2001], as defined in Figure 14a. We also show the methane-synchronized record from the Byrd ice core for reference in Figure 14b [*Blunier and Brook*, 2001]. We compare the model results with the *Siddall et al.* [2003] Red Sea sea level curve on the GRIP SS09 time scale (details of the age model are given in the Figure 14 caption).

[94] We first consider a scenario in which ice volume grows during cold periods and decreases during warm periods. In this scenario, ice continues to grow until the abrupt MIS 4–3 transition in the Greenland record (Figure 14c). There is then a period of melting lasting some 9000 years during the Greenland warm period. This continuous period of melting leads to a lag of 9000 years between the end of the MIS 4 sea level lowstand and the first major MIS 3 sea level highstand. The resulting sea level curve bears little similarity to the MIS 3 stratigraphy defined by the reconstructions discussed in this text and represented by the *Siddall et al.* [2003] Red Sea sea level curve.

[95] We next consider the opposite scenario, where sea level is driven by ice sheet growth during Greenland warm periods (Figure 14d). Despite the very simple approach, this scenario captures the dominant features of the MIS 3 sea level curve. Ice loss commences earlier, and the first MIS 3 sea level highstand occurs very close to its synchronized timing. Interestingly, the period of reduced temperature that precedes the rapid MIS 4–3 transition in Greenland (corresponding with Antarctic warming) also drives sea level to be around 20 m higher in the first half of MIS 3 compared to the latter half, a robust feature of the MIS 3 sea level stratigraphy. By simply invoking an Antarctic-style timing for the MIS 3 sea level record (as in the work by *Siddall et al.* [2003]), we therefore find an alternative explanation for the fact that sea level was higher during the early half of MIS 3 (i.e., alternative to the idea that this would reflect the small change in northern summer insolation forcing through MIS 3).

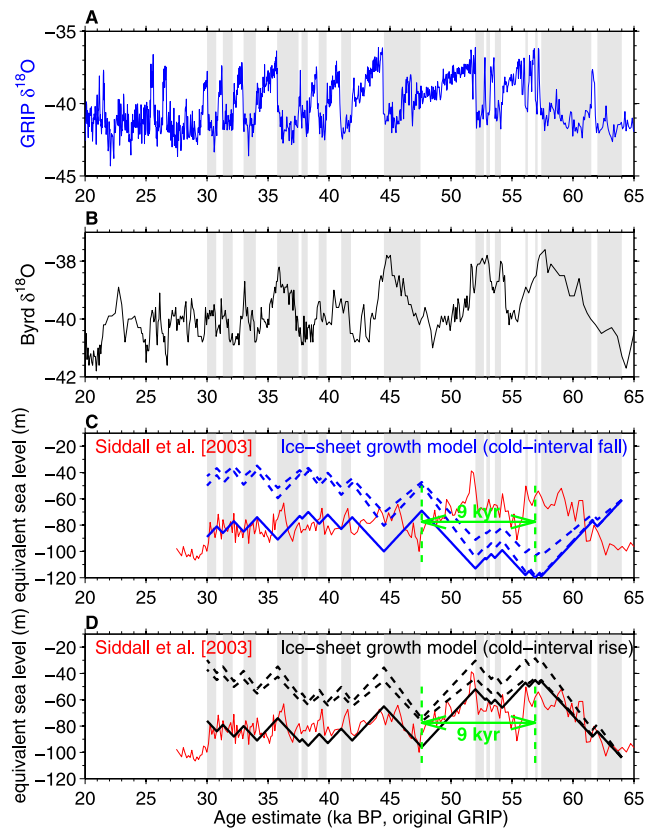


**Figure 14.** The “limiting ice growth model,” a conceptual model, as described in section 6.5. In the plots shown, sea level rises and falls at a rate of  $1 \text{ cm a}^{-1}$ . The (a) GRIP and (b) Byrd  $\delta^{18}\text{O}$  records after *Blunier and Brook* [2001]. All records are on the GRIP time scale. Grey bars represent cold periods in the Greenland time scale. (c) Greenland “cold stadal fall” timing. Ice volume increases (sea level lowers) during cold periods in Greenland and decreases (sea level rises) during warm periods in Greenland. (d) Antarctic “cold stadal rise” timing. Ice volume increases (sea level lowers) during warm periods, and ice volume decreases (sea level rises) during cold periods in Greenland. The  $y$  axes in Figures 14c and 14d are in units of sea level equivalent ice volume. In both Figures 14c and 14d the top dashed line represents the effect of an ice sheet loss rate of  $1.25 \text{ cm a}^{-1}$  compared to a growth rate of  $1 \text{ cm a}^{-1}$ . The bottom dashed line represents the effect of an ice sheet loss rate of  $1 \text{ cm a}^{-1}$  compared to a growth rate of  $0.75 \text{ cm a}^{-1}$ . The original GISP2 age model presented by *Siddall et al.* [2003] is translated onto the GRIP age scale by using tie points at the midpoints of the D-O warmings (i.e., 30, 36.5, 39.5, 41.75, 46.5, and 52.61 ka B.P.).

[96] We now consider the case of a greater rate of ice volume loss than ice volume increase. The dashed lines in Figures 14c and 14d are included to illustrate the effect of making ice sheet loss rate greater than ice sheet growth during MIS 3. In each simulation the top dashed line represents the effect of an ice sheet loss rate of  $1.25 \text{ cm a}^{-1}$  compared to a growth rate of  $1 \text{ cm a}^{-1}$ . The bottom dashed line represents the effect of an ice sheet loss rate of  $1 \text{ cm a}^{-1}$  compared to a growth rate of  $0.75 \text{ cm a}^{-1}$ . Larger ice sheet reduction compared to ice sheet growth leads to a

net loss of ice and a corresponding increase in sea level during MIS 3 for both simulations, in poor correspondence with sea level estimates. This effect is easily explained: the total duration of warm D-O periods in Greenland is very similar to the total duration of cold periods (one could also say the total duration of warming periods in Antarctica is similar to the total duration of cooling periods). Any increase in the rate of ice sheet loss compared to ice sheet growth over this period leads to a net loss of ice volume by the end of MIS 3. Even the relatively subtle asymmetry applied in the sensitivity tests leads to a net ice sheet reduction of 50 m. The ice volume response integrated over the whole of MIS 3 is estimated to be only 20 m. This result would imply that the rate of ice sheet growth was similar to the rate of ice sheet reduction during MIS 3, which may either imply an increase in ice sheet growth during glacial times, a reduction in ice sheet loss, or indeed both. It seems plausible that the inferred similarity in the rates of ice sheet growth and loss during glacial times (MIS 3) reflects more rapid growth of ice sheets under glacial conditions than during interglacials or deglaciations. Equally, the processes underlying the greatly accelerated rates of ice volume loss during glacial terminations may not be analogous to those governing the rates of ice volume loss that episodically occurred during the predominantly glacial conditions of MIS 3; that is, the maximum rate of ice volume loss could be reduced during MIS 3 compared to the termination. We conclude that it is likely that both ice sheet growth rates increased during the glacial period and rates of ice sheet loss reduced in order to generate the observed similarity between ice sheet growth and loss.

[97] Although the various sea level reconstructions disagree on the details of chronology, they do resolve a consensus chronology that is sufficiently constrained to allow testing of the two modeled scenarios, by exploiting the predicted 9000-year difference in the timing of the initial MIS 3 highstand between the two scenarios (Figures 14c and 14d). In the context of this simple, conceptual model of limiting ice sheet growth/loss, all of the available evidence for the timing of the MIS 4–3 sea level transition discussed in section 5 (Figures 10–14) supports the hypothesis that sea level rose during Greenland stadials and fell during interstadials. The other scenario, with sea level rising during Greenland warming [e.g., *Arz et al.*, 2007], is not supported by our simple model. Because cold periods in Greenland correspond to Antarctic warming events [*Blunier and Brook*, 2001], the accepted scenario argues for an Antarctic-type timing of the global sea level/ice volume fluctuations, as previously proposed by *Shackleton et al.* [2000], *Siddall et al.* [2003], and *Rohling et al.* [2004]. As discussed in section 6.4, *Clark et al.* [2007] provide a plausible physical mechanism which can explain this timing of events.

[98] Note that ice sheet and ocean responses operate on different time scales: ocean heat transport is expected to respond rapidly to meltwater pulses [*Stocker et al.*, 1992; *Manabe and Stouffer*, 1997; *Ganopolski and Rahmstorf*, 2001; *Stocker and Johnsen*, 2003; *Knutti et al.*, 2004;

*Schmittner*, 2005], but ice sheets respond on time scales of thousands of years [e.g., *Marshall and Clarke*, 1999; *Bintanja et al.*, 2002; *Arz et al.*, 2007]. If one assumes that MIS 3 ice volume fluctuations drive the D-O cold periods by defining periods of Laurentide melting, then one may anticipate that increases in sea level are closely timed to the D-O cold phases (because of the short response time of ocean circulation to meltwater input). On the other hand, if the D-O cold phases promote ice sheet growth, a more complicated relationship involving a lag of the ice sheet response to temperature change may be expected, and a more sophisticated model might be more appropriate (because of the relatively slow response of ice sheets to temperature change). That our simple model gives such a promising result is best explained therefore if the Greenland temperature proxy record represents a response to melting of the Laurentide ice sheet, rather than the Laurentide ice sheet responding to Greenland temperature. To confirm this result one would need to consider a more sophisticated model which incorporates the lagged response of sea level change to temperature.

### 6.6. Lower-Magnitude Variability

[99] Throughout this text we have concentrated on the large-magnitude variability of the four major sea level fluctuations, which are unambiguously resolved in nearly all of the records presented. The question of an ice volume response to the shorter D-O events or lower-magnitude AA events has not been addressed. Figure 14 makes it clear why it is hard to address this issue with the available data and methods: these events only last around 1 ka, which implies a maximum ice sheet response of 10–20 m (given an ice sheet growth rate of 1–2 cm a<sup>-1</sup>). This does not allow for any time lag in the ice sheet response, and so this is an upper estimate. Both the time scale and magnitude of this response are very difficult to resolve in coral records or down core records of marine oxygen isotopes. Note that none of the records in this paper claim to be able to resolve sea level variations that are less than 12 m in magnitude (at the 2 $\sigma$  uncertainty level). There is some indication from Red Sea records that there is a response to these short events between 40 and 45 ka B.P. (Figures 8 and 9), but this is certainly ambiguous and not yet adequately resolved.

[100] The results of our conceptual model should be regarded with caution in this respect. The model does not include any time lag in the response of ice sheets. If included, this would lead to a smaller response than suggested in Figure 14. In this respect it is crucial to establish whether the model can be considered suggestive of an oceanic response to meltwater input into the Atlantic that led to reduced northward heat transport by the AMOC. If so, then there would be very little lag because the oceanic response to meltwater input is rapid, and the model would suggest that ice sheet fluctuations of the order of 10–20 m may indeed be found in association with short D-O events. If, on the other hand, our conceptual model represents an ice sheet response to temperature variations, then a time lag of thousands of years may need to be applied, which would

greatly reduce the predicted magnitudes of ice sheet response to short D-O events.

## 7. CONCLUSIONS

[101] There are important differences between models of varying complexity on the predicted phasing of ice volume and climate change during MIS 3. Although dating and synchronization techniques continue to improve, considerable uncertainties remain. These uncertainties not only concern the chronology of sea level fluctuations but also arise from the many different age models used for Greenland and Antarctic records [e.g., *Johnsen et al.*, 1995, 2001; *Meese et al.*, 1997; *Shackleton et al.*, 2004; *Andersen et al.*, 2006]. Even well-dated paleoclimate proxy records such as that from Hulu Cave suffer from large variations in growth rate and contain sections where the comparison with Greenland ice core records is ambiguous [*Shackleton et al.*, 2004; *Clark et al.*, 2007]. Regarding radiometrically dated coral samples, the correction of U/Th dates for open system effects remains contentious. Because most sources of uncertainty have been identified, however, we anticipate that many of the chronological issues raised in this paper may be resolved as age models and synchronization techniques improve.

[102] Despite these difficulties we consider that there is important convergence from the various approaches on the magnitude and rate of sea level change during MIS 3:

[103] 1. MIS 3 sea level consisted of an initial rise to a level of approximately –60 m for the first half of MIS 3 and subsequent drop to –80 m for the remainder. This 20 m fall in sea level may either be driven by changes in summer insolation at 65°N or by the fact that an AA-type temperature signal drives ice sheet growth and decay, which followed a similar pattern. Sea level then fell to MIS 2 levels. Only one of the eighteen key records shown here does not show this characteristic stratigraphy.

[104] 2. Superimposed on this are likely four sea level fluctuations of between 20 and 30 m magnitude during MIS 3.

[105] 3. We note that ice sheet growth rates observed over several distinct periods (in addition to observations within MIS 3) are of the magnitude necessary to drive sea level fluctuations of tens of meters during the duration of MIS 3. Rates of sea level change are reproduced in several studies using independent techniques and data and are typically 1–2 cm of sea level equivalent ice sheet growth per year.

[106] 4. All of the recent studies we have considered estimate that the MIS 4 to MIS 3 transition in sea level occurred between 57 and 60 ka B.P., in good agreement with the SPECMAP estimate of 59 ka B.P.

[107] 5. There is a convergence of evidence that sea level rose during cold phases in Greenland and warming periods in Antarctica, supporting the notion of *Chappell* [2002] and *Siddall et al.* [2003] that sea level follows an essentially Antarctic rhythm. This is supported (tentatively) by our conceptual “limiting ice sheet growth/loss model,” which

shows a good resemblance to reconstructed sea level changes despite its obvious simplicity.

[108] Given this last point, the assumption that the temperature history revealed in Greenland ice cores is appropriate to force ice sheet models during MIS 3 should be carefully examined. Fully coupled modeling of the ocean-ice-sheet-atmosphere should be developed, and careful model intercomparison should be carried out. The link between benthic oxygen ratios and sea level is of continued interest. Iterative models comprising a 3-D ocean circulation module combined with a representation of the major ice sheets, which aim to find ice sheet configurations consistent with benthic isotope records from various locations, should be further investigated for high-resolution records of MIS 3. We therefore add a final, more tentative conclusion from this study:

[109] 6. This work suggests that ice volume fluctuated on an Antarctic rhythm during MIS 3; how can this be the case? Recent modeling work [Clark *et al.*, 2007] suggests that the mass balance of the major northern hemisphere ice sheets may be dominated by an Antarctic-like temperature signal at the equatorial Pacific. This might explain the apparent separation of the Greenland temperature signal from the growth pattern of the major Northern Hemisphere ice sheets during MIS 3.

## 8. FUTURE WORK

[110] This review outlines clear directions for further work. These fall into two broad categories: improved observational constraints and new modeling approaches. The scope for new techniques and methods not yet applied to MIS 3 is discussed in sections 3.2 and 3.3, and so we limit our discussion here to advancements in established techniques.

[111] Improvements in dating techniques for speleothem records such as Hulu Cave, improved age constraints on ice core temperature reconstructions, and improved age constraints on coral ages (e.g., by correcting for open system effects and by improvements in analytical techniques) will all play an important role in helping to refine the observational constraints on MIS 3 sea level variations.

[112] As well as improvements in absolute dating, there is scope to derive records with coregistered signals representing both sea level and some independent proxy. Arz *et al.* [2007] and Rohling *et al.* [2008] demonstrated this by considering paleomagnetic intensity and dust flux alongside Red Sea oxygen isotope records. Another example is the benthic isotope record of the Portuguese margin of Shackleton *et al.* [2000], which was synchronized using the planktic oxygen isotope record, which was strikingly similar to Greenland temperature proxies. There is scope to apply this technique to more ocean sediment cores in the future.

[113] In terms of sea level estimates, Chappell [2002] indicated the potential for the modeling of coral terrace formation as a means to develop a rigorous stratigraphic context to better constrain coral-based sea level estimates.

After Siddall *et al.* [2003, 2004] and Arz *et al.* [2007], further work on Red Sea oxygen isotope records as well as the dynamics of the Red Sea response to sea level has potential to better refine the estimates of sea level fluctuations during MIS 3.

[114] The existing data do not sufficiently constrain the relationship between MIS 3 temperature and ice volume fluctuations to allow distinction between competing hypotheses and models. Despite this, existing models and data do make it clear that fluctuations in the ice sheets provoked responses in the ocean heat transport and thereby high-latitude temperature. The combination of coupled modeling efforts with new data will be the key to understanding the climate dynamics during MIS 3, when ice volume and temperature underwent large, abrupt fluctuations.

[115] Many aspects of the observed sea level and broader climate fluctuations during MIS 3 remain poorly understood. In particular the underlying processes that drive the variability are either not represented or misrepresented in the current generation of climate models. Improvements in the representation of ice dynamics [e.g., Alley *et al.*, 2005] and the coupling of ice-ocean-atmosphere systems within models which are capable of millennial-transient simulations will be an important aspect of future work.

[116] **ACKNOWLEDGMENTS.** Suggestions and contributions of data from Nick Shackleton, Jerry McManus, Dick Peltier, Helge Arz, Peter Huybers, Thomas Stocker, Peter Clark, and Thomas Blunier were useful in bringing together this document, although the text does not necessarily represent their opinions. Mark Siddall is supported by a Lamont-Doherty research fellowship. This paper contributes to UK Natural Environment Research Council projects NE/C003152/1, NER/T/S/2002/00453, and NE/D001773/1. William G. Thompson is supported by grants from the National Science Foundation (OCE-0602383) and the Ocean and Climate Change Institute of Woods Hole Oceanographic Institution. Claire Waelbroeck was supported by EC grant EVK-2000-00089, by the CNRS, CEA, and IPEV, as well as the IMAGES program.

[117] The Editor responsible for this paper was Henk Dijkstra. He thanks Thorsten Kiefer, Peter Clark, and R. S. W. van de Wal as the technical reviewers along with one anonymous technical reviewer.

## REFERENCES

- Adkins, J. F., and D. P. Schrag (2003), Reconstructing Last Glacial Maximum bottom water salinities from deep-sea sediment pore fluid profiles, *Earth Planet. Sci. Lett.*, *216*, 109–123, doi:10.1016/S0012-821X(03)00502-8.
- Adkins, J. F., K. McIntyre, and D. P. Schrag (2002), The salinity, temperature and  $\delta^{18}\text{O}$  content of the glacial deep ocean, *Science*, *298*, 1769–1773, doi:10.1126/science.1076252.
- Alley, R. B., and P. U. Clark (1999), The deglaciation of the Northern Hemisphere: A global perspective, *Annu. Rev. Earth Planet. Sci.*, *27*, 149–182, doi:10.1146/annurev.earth.27.1.149.
- Alley, R. B., S. Anandakrishnan, and P. Jung (2001), Stochastic resonance in the North Atlantic, *Paleoceanography*, *16*(2), 190–198, doi:10.1029/2000PA000518.
- Alley, R. B., P. U. Clark, P. Huybrechts, and I. Joughin (2005), Ice-sheet and sea-level changes, *Science*, *310*, 456–460, doi:10.1126/science.1114613.



- Almogi-Labin, A., C. Hemleben, D. Meischner, and H. Erlenkeuser (1991), Paleoenvironmental events during the last 13,000 years in the central Red Sea as recorded by pteropoda, *Paleoceanography*, *6*, 83–98, doi:10.1029/90PA01881.
- Andersen, K. K., et al. (2006), The Greenland Ice Core Chronology 2005, 15–42 ka. Part 1: Constructing the time scale, *Quat. Sci. Rev.*, *25*(23–24), 3246–3257, doi:10.1016/j.quascirev.2006.08.002.
- Andrews, J. T., and M. A. W. Mahaffy (1976), Growth rate of the Laurentide ice sheet and sea level lowering (with emphasis on the 115,000 BP sea level low), *Quat. Res.*, *6*(2), 167–183, doi:10.1016/0033-5894(76)90048-X.
- Arz, H. W., J. Pätzold, P. J. Müller, and M. O. Moammer (2003a), Influence of Northern Hemisphere climate and global sea level rise on the restricted Red Sea marine environment during termination I, *Paleoceanography*, *18*(2), 1053, doi:10.1029/2002PA000864.
- Arz, H. W., F. Lamy, J. Pätzold, P. J. Müller, and M. Prins (2003b), Mediterranean moisture source for an Early Holocene humid period in the northern Red Sea, *Science*, *300*, 118–121, doi:10.1126/science.1080325.
- Arz, H. W., F. Lamy, A. Ganopolski, N. Nowaczyk, and J. Pätzold (2007), Dominant Northern Hemisphere climate control over millennial-scale glacial sea-level variability, *Quat. Sci. Rev.*, *26*(3–4), 312–321, doi:10.1016/j.quascirev.2006.07.016.
- Bard, E., and M. Frank (2006), Climate change and solar variability: What's new under the sun?, *Earth Planet. Sci. Lett.*, *248*, 1–14, doi:10.1016/j.epsl.2006.06.016.
- Bard, E., B. Hamelin, M. Arnold, L. Montaggioni, G. Cabioch, G. Faure, and F. Rougerie (1996), Sea level record from Tahiti corals and the timing of deglacial meltwater discharge, *Nature*, *382*, 241–244, doi:10.1038/382241a0.
- Bassinot, F. C., L. D. Labeyrie, E. Vincent, X. Quidelleur, N. J. Shackleton, and Y. Lancelot (1994), The astronomical theory of climate and the age of the Bruhnes-Matuyama magnetic reversal, *Earth Planet. Sci. Lett.*, *126*, 91–108, doi:10.1016/0012-821X(94)90244-5.
- Bintanja, R., R. S. W. van de Wal, and J. Oerlemans (2002), Global ice volume variations through the last glacial cycle simulated by a 3-D ice-dynamical model, *Quat. Int.*, *95–95*, 11–23, doi:10.1016/S1040-6182(02)00023-X.
- Bintanja, R., R. S. W. van de Wal, and J. Oerlemans (2005), Modelled atmospheric temperatures and global sea levels over the past million years, *Nature*, *437*, 125–128, doi:10.1038/nature03975.
- Bloom, A. L. (1967), Pleistocene shorelines—A new test of isostasy, *Geol. Soc. Am. Bull.*, *78*(12), 1477–1494, doi:10.1130/0016-7606(1967)78[1477:PSANTO]2.0.CO;2.
- Blunier, T., and E. Brook (2001), Timing of millennial-scale climate change in Antarctica and Greenland during the last glacial period, *Science*, *291*, 109–112, doi:10.1126/science.291.5501.109.
- Blunier, T., et al. (1998), Asynchrony of Antarctica and Greenland climate during the last glacial, *Nature*, *394*, 739–743, doi:10.1038/29447.
- Bond, G. C., and R. Lotti (1995), Iceberg discharges into the North-Atlantic on millennial time scales during the last glaciation, *Science*, *267*(5200), 1005–1010, doi:10.1126/science.267.5200.1005.
- Bond, G., W. Showers, M. Cheseby, R. Lotti, P. Almasi, P. deMenocal, P. Priore, H. Cullen, I. Hajdas, and G. Bonani (1997), A pervasive millennial-scale cycle in North Atlantic Holocene and glacial climates, *Science*, *278*(5341), 1257–1266, doi:10.1126/science.278.5341.1257.
- Bond, G. C., B. Kromer, J. Beer, R. Muscheler, M. N. Evans, W. Showers, S. Hoffmann, R. Lotti-Bond, I. Hajdas, and G. Bonani (2001), Persistent solar influence on north Atlantic climate during the Holocene, *Science*, *294*(5549), 2130–2136, doi:10.1126/science.1065680.
- Braun, H., M. Christl, S. Rahmstorf, A. Ganopolski, A. Mangini, C. Kubatzki, K. Roth, and B. Kromer (2005), Possible solar origin of the 1,470-year glacial climate cycle demonstrated in a coupled model, *Nature*, *438*(7065), 208–211, doi:10.1038/nature04121.
- Broecker, W. S., D. M. Peteet, and D. Rind (1985), Does the ocean-atmosphere system have more than one stable mode of operation?, *Nature*, *315*, 21–26, doi:10.1038/315021a0.
- Burns, S. J., D. Fleitmann, A. Matter, J. Kramers, and A. A. Al-Subbary (2003), Indian Ocean climate and an absolute chronology over Dansgaard/Oeschger events 9 to 13, *Science*, *301*(5638), 1365–1367, doi:10.1126/science.1086227.
- Chappell, J. (2002), Sea level changes forced ice breakouts in the Last Glacial Cycle: New results from coral terraces, *Quat. Sci. Rev.*, *21*(10), 1229–1240, doi:10.1016/S0277-3791(01)00141-X.
- Chappell, J., and N. J. Shackleton (1986), Oxygen isotopes and sea-level, *Nature*, *324*(6093), 137–140, doi:10.1038/324137a0.
- Chappell, J., A. Omura, T. Esat, M. McCulloch, J. Pandolfi, Y. Ota, and B. Pillans (1996), Reconciliation of late Quaternary sea levels derived from coral terraces at Huon Peninsula with deep sea oxygen isotope records, *Earth Planet. Sci. Lett.*, *141*(1–4), 227–236.
- Clark, P. U., R. B. Alley, and D. Pollard (1999), Northern Hemisphere ice-sheet influences on global climate change, *Science*, *286*, 1104–1111, doi:10.1126/science.286.5442.1104.
- Clark, P. U., S. J. Marshall, G. K. C. Clarke, S. W. Hostetler, J. M. Licciardi, and J. T. Teller (2001), Freshwater forcing of abrupt climate change during the last glaciation, *Science*, *293*, 283–287, doi:10.1126/science.1062517.
- Clark, P. U., N. G. Piasias, T. F. Stocker, and A. J. Weaver (2002), The role of the thermohaline circulation in abrupt climate change, *Nature*, *415*, 863–869, doi:10.1038/415863a.
- Clark, P. U., S. W. Hostetler, N. G. Piasias, A. Schmittner, and K. J. Meissner (2007), Mechanisms for a ~7-kyr climate and sea-level oscillation during marine isotope stage 3, in *Ocean Circulation: Mechanisms and Impacts*, *Geophys. Monogr. Ser.*, vol. 173, edited by A. Schmittner, J. Chiang, and S. Hemmings, pp. 209–246, AGU, Washington, D. C.
- Curry, W. B., and D. W. Oppo (2005), Glacial water mass geometry and the distribution of  $\delta^{13}\text{C}$  of  $\Sigma\text{CO}_2$  in the western Atlantic Ocean, *Paleoceanography*, *20*, PA1017, doi:10.1029/2004PA001021.
- Cutler, K. B., R. L. Edwards, F. W. Taylor, H. Cheng, J. Adkins, C. D. Gallup, P. M. Cutler, G. S. Burr, and A. L. Bloom (2003), Rapid sea-level fall and deep-ocean temperature change since the last interglacial period, *Earth Planet. Sci. Lett.*, *206*(3–4), 253–271, doi:10.1016/S0012-821X(02)01107-X.
- Dannenmann, S., B. K. Linsley, D. W. Oppo, Y. Rosenthal, and L. Beaufort (2003), East Asian monsoon forcing of suborbital variability in the Sulu Sea during marine isotope stage 3: Link to Northern Hemisphere climate, *Geochem. Geophys. Geosyst.*, *4*(1), 1001, doi:10.1029/2002GC000390.
- Dansgaard, W. (1964), Stable isotopes in precipitation, *Tellus*, *16*(4), 436–468.
- Dansgaard, W., S. J. Johnsen, H. B. Clausen, D. Dahl-Jensen, N. Gundestrup, C. U. Hammer, and H. Oeschger (1984), North Atlantic climatic oscillations revealed by deep Greenland ice cores, in *Climate Processes and Climate Sensitivity*, *Geophys. Monogr. Ser.*, vol. 29, edited by J. E. Hansen and T. Takahashi, pp. 288–298, AGU, Washington, D. C.
- Delmotte, M., J. Chappellaz, E. Brook, P. Yiou, J. M. Barnola, C. Goujon, D. Raynaud, and V. I. Lipenkov (2004), Atmospheric methane during the last four glacial-interglacial cycles: Rapid changes and their link with Antarctic temperature, *J. Geophys. Res.*, *109*, D12104, doi:10.1029/2003JD004417.
- Denton, G. H., R. B. Alley, G. C. Comer, and W. S. Broecker (2005), The role of seasonality in abrupt climate change, *Quat. Sci. Rev.*, *24*(10–11), 1159–1182, doi:10.1016/j.quascirev.2004.12.002.
- Deuser, W. G., E. H. Ross, and L. S. Waterman (1976), Glacial and pluvial periods: Their relationship revealed by Pleistocene sediments of the Red Sea and Gulf of Aden, *Science*, *191*(4232), 1168–1170, doi:10.1126/science.191.4232.1168.

- Ditlevsen, P. D. (1999), Observation of alpha-stable noise induced millennial climate changes from an ice-core record, *Geophys. Res. Lett.*, 26(10), 1441–1444, doi:10.1029/1999GL900252.
- Ditlevsen, P. D., M. S. Kristensen, and K. K. Andersen (2005), The recurrence time of Dansgaard-Oeschger events and limits on the possible periodic component, *J. Clim.*, 18(14), 2594–2603, doi:10.1175/JCLI3437.1.
- Duplessy, J. C. (2004), Global ocean circulation and its past variations, *C. R. Geosci.*, 336(7–8), 657–666, doi:10.1016/j.crte.2003.12.021.
- EPICA Community Members (2006), One-to-one interhemispheric coupling of polar climate variability during the last glacial, *Nature*, 444, 195–198, doi:10.1038/nature05301.
- Esat, T. M., and Y. Yokoyama (2002), Rapid sea-level, ice-volume and radiocarbon excursions during a Heinrich event at Huon Peninsula, *Geochim. Cosmochim. Acta*, 66(15A), A216–A216.
- Esat, T. M., and Y. Yokoyama (2006), Growth patterns of the last ice age coral terraces at Huon Peninsula, *Global Planet. Change*, 54(3–4), 216–224, doi:10.1016/j.gloplacha.2006.06.020.
- Esat, T. M., M. T. McCulloch, J. Chappell, B. Pillans, and A. Omura (1999), Rapid fluctuations in sea level recorded at Huon Peninsula during the penultimate deglaciation, *Science*, 283(5399), 197–201, doi:10.1126/science.283.5399.197.
- Fairbanks, R. G. (1989), A 17,000 year glacio-eustatic sea level record: Influence of glacial melting rates on the Younger Dryas event and deep ocean circulation, *Nature*, 342, 637–642, doi:10.1038/342637a0.
- Fairbanks, R. G., R. A. Mortlock, T.-C. Chiu, L. Cao, A. Kaplan, T. P. Guilderson, T. W. Fairbanks, and A. L. Bloom (2005), Marine radiocarbon calibration curve spanning 10,000 to 50,000 years B.P. based on paired  $^{230}\text{Th}/^{234}\text{U}/^{238}\text{U}$  and  $^{14}\text{C}$  dates on pristine corals, *Quat. Sci. Rev.*, 24, 1781–1796, doi:10.1016/j.quascirev.2005.04.007.
- Fenton, M., S. Geiselsart, E. J. Rohling, and C. Hemleben (2000), Aplanktonic zones in the Red Sea, *Mar. Micropaleontol.*, 40, 277–294, doi:10.1016/S0377-8398(00)00042-6.
- Fernandes, C. A. R., E. J. Rohling, and M. Siddall (2006), Absence of post-Miocene Red Sea land bridges: Biogeographic implications, *J. Biogeogr.*, 33, 961–966, doi:10.1111/j.1365-2699.2006.01478.x.
- Flückiger, J., R. Knutti, and J. W. C. White (2006), Oceanic processes as potential trigger and amplifying mechanisms for Heinrich events, *Paleoceanography*, 21, PA2014, doi:10.1029/2005PA001204.
- Gallup, C. D., R. L. Edwards, and R. G. Johnson (1994), The timing of high sea levels over the past 200,000 years, *Science*, 263(5148), 796–800, doi:10.1126/science.263.5148.796.
- Ganopolski, A., and S. Rahmstorf (2001), Simulation of rapid glacial climate changes in a coupled climate model, *Nature*, 409, 153–158, doi:10.1038/35051500.
- Groote, P. M., and M. Stuiver (1997), Oxygen 18/16 variability in Greenland snow and ice with  $10^{-3}$ - to  $10^3$ -year time resolution, *J. Geophys. Res.*, 102(C12), 26,455–26,470.
- Hanebuth, T. J. J., Y. Saito, S. Tanabe, Q. L. Vu, and Q. T. Ngo (2006), Sea levels during late marine isotope stage 3 (or older?) reported from the Red River delta (northern Vietnam) and adjacent regions, *Quat. Int.*, 145–146, 119–134, doi:10.1016/j.quaint.2005.07.008.
- Haq, B. U., J. Hardenbol, and P. R. Vail (1987), Chronology of fluctuating sea levels since the Triassic, *Science*, 235(4793), 1156–1167, doi:10.1126/science.235.4793.1156.
- Heinrich, H. (1988), Origin and consequences of cyclic ice rafting in the northeast Atlantic ocean during the past 130,000 years, *Quat. Res.*, 29(2), 142–152, doi:10.1016/0033-5894(88)90057-9.
- Hemleben, C., D. Meischner, R. Zahn, A. Almogi, H. Labin, B. Erlenkeuser, and B. Hiller (1996), Three hundred eighty thousand year long stable isotope and faunal records from the Red Sea: Influence of global sea level change on hydrography, *Paleoceanography*, 11(2), 147–156, doi:10.1029/95PA03838.
- Hemming, S. R. (2004), Heinrich events: Massive late Pleistocene detritus layers of the North Atlantic and their global climate imprint, *Rev. Geophys.*, 42, RG1005, doi:10.1029/2003RG000128.
- Hill, H. W., B. P. Flower, T. M. Quinn, D. J. Hollander, and T. P. Guilderson (2006), Laurentide Ice Sheet meltwater and abrupt climate change during the last glaciation, *Paleoceanography*, 21, PA1006, doi:10.1029/2005PA001186.
- Huber, C., M. Leuenberger, R. Spahni, J. Flückiger, J. Schwander, T. F. Stocker, S. J. Johnsen, A. Landais, and J. Jouzel (2006), Isotope calibrated Greenland temperature record over marine isotope stage 3 and its relation to  $\text{CH}_4$ , *Earth Planet. Sci. Lett.*, 243, 504–519, doi:10.1016/j.epsl.2006.01.002.
- Huybers, P. (2006), Early Pleistocene glacial cycles and the integrated summer insolation forcing, *Science*, 313, 508–511, doi:10.1126/science.1125249.
- Huybers, P., and C. Wunsch (2004), A depth-derived Pleistocene age model: Uncertainty estimates, sedimentation variability, and nonlinear climate change, *Paleoceanography*, 19, PA1028, doi:10.1029/2002PA000857.
- Imbrie, J., and K. P. Imbrie (1979), *Ice Ages, Solving the Mystery*, Harvard Univ. Press, Cambridge, Mass.
- Imbrie, J., J. D. Hays, D. G. Martinson, A. McIntyre, A. C. Mix, J. J. Morley, N. G. Pisias, W. L. Prell, and N. J. Shackleton (1984), The orbital theory of Pleistocene climate: Support from a revised chronology of the marine  $\delta^{18}\text{O}$  record, in *Milankovitch and Climate, Part 1*, edited by A. L. Berger et al., pp. 269–305, D. Reidel, Dordrecht, Netherlands.
- Ivanova, E. V. (1985), Late Quaternary biostratigraphy and paleotemperatures of the Red Sea and the Gulf of Aden based on planktonic-foraminifera and pteropods, *Mar. Micropaleontol.*, 9(4), 335–364, doi:10.1016/0377-8398(85)90003-9.
- Johnsen, S. J., W. Dansgaard, H. B. Clausen, and C. C. Langway Jr. (1972), Oxygen isotope profiles through the Antarctic and Greenland ice sheets, *Nature*, 235(5339), 429–434, doi:10.1038/235429a0.
- Johnsen, S. J., H. B. Clausen, W. Dansgaard, N. S. Gundestrup, C. U. Hammer, and H. Tauber (1995), The EEM stable-isotope record along the GRIP ice core and its interpretation, *Quat. Res.*, 43(2), 117–124, doi:10.1006/qres.1995.1013.
- Johnsen, S. J., D. Dahl-Jensen, N. Gundestrup, J. P. Steffensen, H. B. Clausen, H. Miller, V. Masson-Delmotte, A. E. Sveinbjornsdottir, and J. White (2001), Oxygen isotope and palaeotemperature records from six Greenland ice-core stations: Camp Century, Dye-3, GRIP, GISP2, Renland and NorthGRIP, *J. Quat. Sci.*, 16(4), 299–307, doi:10.1002/jqs.622.
- Johnston, P. (1993), The effect of spatially nonuniform water loads on prediction of sea-level change, *Geophys. J. Int.*, 114(3), 615–634, doi:10.1111/j.1365-246X.1993.tb06992.x.
- Jouet, G., S. Berne, M. Rabineau, M. A. Bassetti, P. Bernier, B. Dennielou, F. J. Sierro, J. A. Flores, and M. Taviani (2006), Shoreface migrations at the shelf edge and sea-level changes around the Last Glacial Maximum (Gulf of Lions, NW Mediterranean), *Mar. Geol.*, 234(1–4), 21–42, doi:10.1016/j.margeo.2006.09.012.
- Keeling, R. F., and M. Visbeck (2005), Northern ice discharges and Antarctic warming: Could ocean eddies provide the link?, *Quat. Sci. Rev.*, 24(16–17), 1809–1820, doi:10.1016/j.quascirev.2005.04.005.
- Kim, S. T., and J. R. O'Neil (1997), Equilibrium and nonequilibrium oxygen isotope effects in synthetic calcites, *Geochim. Cosmochim. Acta*, 61, 3461–3475, doi:10.1016/S0016-7037(97)00169-5.
- Knutti, R., J. Flückiger, T. F. Stocker, and A. Timmermann (2004), Strong hemispheric coupling of glacial climate through freshwater discharge and ocean circulation, *Nature*, 430, 851–856, doi:10.1038/nature02786.
- Labeyrie, L. D., J. C. Duplessy, and P. L. Blanc (1987), Variations in mode of formation and temperature of oceanic deep waters

- over the past 125,000 years, *Nature*, 327, 477–482, doi:10.1038/327477a0.
- Labeurye, L., C. Waelbroeck, E. Cortijo, E. Michel, and J. C. Duplessy (2005), Changes in deep water hydrology during the last deglaciation, *C. R. Geosci.*, 337(10–11), 919–927, doi:10.1016/j.crte.2005.05.010.
- Laj, C., C. Kissel, A. Mazaud, J. E. T. Channell, and J. Beer (2000), North Atlantic palaeointensity stack since 75 ka (NA-PIS-75) and the duration of the Laschamp event, *Philos. Trans. R. Soc. London, Ser. A*, 358, 1009–1025.
- Lambeck, K., T. M. Esat, and E. K. Potter (2002), Links between climate and sea levels for the past three million years, *Nature*, 419(6903), 199–206, doi:10.1038/nature01089.
- Lea, D. W., P. A. Martin, D. K. Pak, and H. J. Spero (2002), Reconstructing a 350 ky history of sea level using planktonic Mg/Ca and oxygen isotope records from a Cocos Ridge core, *Quat. Sci. Rev.*, 21, 283–293, doi:10.1016/S0277-3791(01)00081-6.
- Leduc, G., L. Vidal, K. Tachikawa, F. Rostek, C. Sonzogni, L. Beaufort, and E. Bard (2007), Moisture transport across Central America as a positive feedback on abrupt climatic changes, *Nature*, 445, 908–911, doi:10.1038/nature05578.
- Lekens, W. A. H., H. P. Sejrup, H. Hafliason, J. Knies, and T. Richter (2006), Meltwater and ice rafting in the southern Norwegian Sea between 20 and 40 calendar kyr BP: Implications for Fennoscandian Heinrich events, *Paleoceanography*, 21, PA3013, doi:10.1029/2005PA001228.
- Li, C., D. S. Battisti, D. P. Schrag, and E. Tziperman (2005), Abrupt climate shifts in Greenland due to displacements of the sea ice edge, *Geophys. Res. Lett.*, 32, L19702, doi:10.1029/2005GL023492.
- Linsley, B. K. (1996), Oxygen isotope evidence of sea level and climatic variations in the Sulu Sea over the past 150,000 years, *Nature*, 380, 234–237, doi:10.1038/380234a0.
- Lisiecki, L. E., and M. E. Raymo (2005), A Pliocene-Pleistocene stack of 57 globally distributed benthic  $\delta^{18}\text{O}$  records, *Paleoceanography*, 20, PA1003, doi:10.1029/2004PA001071.
- Locke, S., and R. C. Thunell (1988), The paleoceanographic record of the last glacial interglacial cycle in the Red Sea and Gulf of Aden, *Palaeogeogr. Palaeoclimatol. Palaeoecol.*, 64(3–4), 163–187, doi:10.1016/0031-0182(88)90005-3.
- Manabe, S., and R. J. Stouffer (1997), Coupled ocean-atmosphere model response to freshwater input: Comparison to Younger Dryas event, *Paleoceanography*, 12, 321–336, doi:10.1029/96PA03932.
- Marshall, S. J., and G. K. C. Clarke (1999), Modeling North American freshwater runoff through the last glacial cycle, *Quat. Res.*, 52(3), 300–315, doi:10.1006/qres.1999.2079.
- Martinson, D. G., N. G. Pisias, J. D. Hays, J. Imbrie, T. C. Moore Jr., and N. J. Shackleton (1987), Age dating and the orbital theory of the ice ages development of a high-resolution 0 to 300,000-year chronostratigraphy, *Quat. Res.*, 27, 1–29, doi:10.1016/0033-5894(87)90046-9.
- Mayewski, P. A., L. D. Meeker, M. S. Twickler, S. Whitlow, Q. Z. Yang, W. B. Lyons, and M. Prentice (1997), Major features and forcing of high-latitude Northern Hemisphere atmospheric circulation using a 110,000-year-long glaciochemical series, *J. Geophys. Res.*, 102(C12), 26,345–26,366, doi:10.1029/96JC03365.
- McManus, J. F., D. W. Oppo, and J. L. Cullen (1999), A 0.5-million-year record of millennial-scale climate variability in the North Atlantic, *Science*, 283(5404), 971–975, doi:10.1126/science.283.5404.971.
- Meese, D. A., A. J. Gow, R. B. Alley, G. A. Zielinski, P. M. Grootes, M. Ram, K. C. Taylor, P. A. Mayewski, and J. F. Bolzan (1997), The Greenland Ice Sheet Project 2 depth-age scale: Methods and results, *J. Geophys. Res.*, 102(C12), 26,411–26,423, doi:10.1029/97JC00269.
- Miller, K. G., M. A. Kominz, J. V. Browning, J. D. Wright, G. S. Mountain, M. E. Katz, P. J. Sugarman, B. S. Cramer, N. Christe-Blick, and S. F. Pekar (2005), The Phanerozoic record of global sea-level change, *Science*, 310(5752), 1293–1298, doi:10.1126/science.1116412.
- Milliman, J. D., D. A. Ross, and T. L. Ku (1969), Precipitation and lithification of deep-sea carbonates in the Red Sea, *J. Sediment. Res.*, 39(2), 724–736.
- Milne, G. A., J. X. Mitrovica, and J. L. Davis (1999), Near-field hydro-isostasy: The implementation of a revised sea-level equation, *Geophys. J. Int.*, 139(2), 464–482, doi:10.1046/j.1365-246x.1999.00971.x.
- Muscheler, R., R. Beer, P. W. Kubik, and H. A. Synal (2005), Geomagnetic field intensity during the last 60,000 years based on  $^{10}\text{Be}$  and  $^{36}\text{Cl}$  from the Summit ice cores and  $^{14}\text{C}$ , *Quat. Sci. Rev.*, 24(16–17), 1849–1860, doi:10.1016/j.quascirev.2005.01.012.
- Ninnemann, U. S., C. D. Charles, and D. A. Hodell (1999), Origin of global millennial scale climate events: Constraints from the Southern Ocean deep sea sedimentary record, in *Mechanisms of Global Climate Change at Millennial Time Scales*, *Geophys. Monogr. Ser.*, vol. 112, edited by P. U. Clark, R. S. Webb, and L. D. Keigwin, pp. 99–112, AGU, Washington, D. C.
- Oppo, D. W., J. F. McManus, and J. L. Cullen (1998), Abrupt climate events 500,000 to 340,000 years ago: Evidence from subpolar north Atlantic sediments, *Science*, 279(5355), 1335–1338, doi:10.1126/science.279.5355.1335.
- Pahnke, K., and R. Zahn (2005), Southern Hemisphere water mass conversion linked with North Atlantic climate variability, *Science*, 307(5716), 1741–1746, doi:10.1126/science.1102163.
- Pahnke, K., R. Zahn, H. Elderfield, and M. Schulz (2003), 340,000-year centennial-scale marine record of Southern Hemisphere climatic oscillation, *Science*, 301(5635), 948–952, doi:10.1126/science.1084451.
- Peltier, W. R., and R. G. Fairbanks (2006), Global glacial ice volume and Last Glacial Maximum duration from an extended Barbados sea level record, *Quat. Sci. Rev.*, 25, 3322–3337, doi:10.1016/j.quascirev.2006.04.010.
- Petit, J. R., et al. (1999), Climate and atmospheric history of the past 420,000 years from the Vostok ice core, Antarctica, *Nature*, 399(6735), 429–436.
- Rahmstorf, S. (2002), Ocean circulation and climate during the past 120,000 years, *Nature*, 419, 207–214, doi:10.1038/nature01090.
- Rahmstorf, S. (2003), Timing of abrupt climate change: A precise clock, *Geophys. Res. Lett.*, 30(10), 1510, doi:10.1029/2003GL017115.
- Rahmstorf, S., and R. B. Alley (2002), Stochastic resonance in glacial climate, *Eos Trans. AGU*, 83(12), 129–135, doi:10.1029/2002EO000078.
- Rasmussen, S. O., et al. (2006), A new Greenland ice core chronology for the last glacial termination, *J. Geophys. Res.*, 111, D06102, doi:10.1029/2005JD006079.
- Reimer, P. J., et al. (2006), IntCal04 terrestrial radiocarbon age calibration, 0–26 cal kyr BP, *Radiocarbon*, 46(3), 1029–1058.
- Reiss, Z., B. Luz, A. Almogi-Labin, E. Halicz, A. Winter, M. Wolf, and D. A. Ross (1980), Late Quaternary paleoceanography of the Gulf of Aqaba (Elat), Red Sea, *Quat. Res.*, 14(3), 294–308, doi:10.1016/0033-5894(80)90013-7.
- Roberts, A. P., and M. Winklhofer (2004), Why are geomagnetic excursions not always recorded in sediments? Constraints from post-depositional remanent magnetization lock-in modelling, *Earth Planet. Sci. Lett.*, 227(3–4), 345–359, doi:10.1016/j.epsl.2004.07.040.
- Roche, D., C. Paillard, and E. Cortijo (2004), Constraints on the duration and freshwater release of Heinrich event 4 through isotope modelling, *Nature*, 432(7015), 379–382, doi:10.1038/nature03059.
- Rohling, E. J. (1994), Glacial conditions in the Red Sea, *Paleoceanography*, 9, 653–660, doi:10.1029/94PA01648.
- Rohling, E. J. (1999), Environmental controls on salinity and  $\delta^{18}\text{O}$  in the Mediterranean, *Paleoceanography*, 14, 706–715, doi:10.1029/1999PA900042.

- Rohling, E. J., and G. R. Bigg (1998), Paleo-salinity and  $\delta^{18}\text{O}$ : A critical assessment, *J. Geophys. Res.*, *103*, 1307–1318, doi:10.1029/97JC01047.
- Rohling, E. J., and S. Cooke (1999), Stable oxygen and carbon isotope ratios in foraminiferal carbonate, in *Modern Foraminifera*, edited by B. K. Sen Gupta, chap. 14, pp. 239–258, Kluwer Acad., Dordrecht, Netherlands.
- Rohling, E. J., M. Fenton, F. J. Jorissen, P. Bertrand, G. Ganssen, and J. P. Caulet (1998), Magnitudes of sea-level lowstands of the past 500,000 years, *Nature*, *394*, 162–165, doi:10.1038/28134.
- Rohling, E. J., P. A. Mayewski, and P. Challenor (2003), On the timing and mechanism of millennial-scale climate variability during the last glacial cycle, *Clim. Dyn.*, *20*, 257–267.
- Rohling, E. J., R. Marsh, N. C. Wells, M. Siddall, and N. R. Edwards (2004), Similar meltwater contributions to glacial sea level changes from Antarctic and northern ice sheets, *Nature*, *430*, 1016–1021, doi:10.1038/nature02859.
- Rohling, E. J., K. Grant, C. Hemleben, M. Kucera, A. P. Roberts, I. Schmeltzer, H. Schulz, M. Siccha, M. Siddall, and G. Trommer (2008), New constraints on the timing of sea level fluctuations during early to middle marine isotope stage 3, *Paleoceanography*, *23*, PA3219, doi:10.1029/2008PA001617.
- Samthein, M., R. Gersonde, S. Niebler, U. Pflaumann, R. Spielhagen, J. Thiede, G. Wefer, and M. Weinelt (2003), Overview of Glacial Atlantic Ocean Mapping (GLAMAP 2000), *Paleoceanography*, *18*(2), 1030, doi:10.1029/2002PA000769.
- Schaefer, J. M., G. H. Denton, D. J. A. Barrell, S. Ivy-Ochs, P. W. Kubik, B. G. Andersen, F. M. Phillips, T. V. Lowell, and C. Schluchter (2006), Near-synchronous interhemispheric termination of the last glacial maximum in mid-latitudes, *Science*, *312*(5779), 1510–1513, doi:10.1126/science.1122872.
- Schiller, A., U. Mikolajewicz, and R. Voss (1997), The stability of the North Atlantic thermohaline circulation in a coupled ocean-atmosphere general circulation model, *Clim. Dyn.*, *13*, 325–347, doi:10.1007/s003820050169.
- Schmidt, G. A. (1999), Forward modeling of carbonate proxy data from planktonic foraminifera using oxygen isotope tracers in a global ocean model, *Paleoceanography*, *14*(4), 482–497, doi:10.1029/1999PA900025.
- Schmittner, A. (2005), Decline of the marine ecosystem caused by a reduction in the Atlantic overturning circulation, *Nature*, *434*, 628–633, doi:10.1038/nature03476.
- Schulz, H., U. von Rad, and H. Erlenkeuser (1998), Correlation between Arabian Sea and Greenland climate oscillations of the past 110,000 years, *Nature*, *393*(6680), 54–57.
- Schulz, M. (2002), On the 1470-year pacing of Dansgaard-Oeschger warm events, *Paleoceanography*, *17*(2), 1014, doi:10.1029/2000PA000571.
- Seager, R., and D. S. Battisti (2007), Challenges to our understanding of the general circulation: Abrupt climate change, in *Global Circulation of the Atmosphere*, edited by T. Schneider and A. H. Sobel, pp. 331–371, Princeton Univ. Press, Princeton, N. J.
- Seager, R., D. S. Battisti, J. Yin, N. Gordon, N. Naik, A. C. Clement, and M. A. Cane (2002), Is the Gulf Stream responsible for Europe's mild winters?, *Q. J. R. Meteorol. Soc.*, *Part B*, *128*(586), 2563–2586, doi:10.1256/qj.01.128.
- Shackleton, N. J. (1987), Oxygen isotopes, ice volume and sea level, *Quat. Sci. Rev.*, *6*, 183–190, doi:10.1016/0277-3791(87)90003-5.
- Shackleton, N. J. (2000), The 100,000 year ice-age cycle identified and found to lag temperature, carbon dioxide and orbital eccentricity, *Science*, *289*, 1897–1902, doi:10.1126/science.289.5486.1897.
- Shackleton, N. J., and N. D. Opdyke (1973), Oxygen isotope and paleomagnetic stratigraphy of equatorial Pacific core V28–238: Oxygen isotope temperatures and ice volumes on a 105 and 106 year scale, *Quat. Res.*, *3*, 39–55, doi:10.1016/0033-5894(73)90052-5.
- Shackleton, N. J., M. A. Hall, and E. Vincent (2000), Phase relationships between millennial-scale events 64,000–24,000 years ago, *Paleoceanography*, *15*, 565–569, doi:10.1029/2000PA000513.
- Shackleton, N. J., R. G. Fairbanks, T.-C. Chiu, and F. Parrenin (2004), Absolute calibration of the Greenland time scale: Implications for Antarctic time scales and for  $\Delta^{14}\text{C}$ , *Quat. Sci. Rev.*, *23*, 1513–1522, doi:10.1016/j.quascirev.2004.03.006.
- Siddall, M., D. A. Smeed, E. J. Rohling, and S. Mathiessen (2002), Modelling the seasonal cycle of the exchange flow in the Straits of Bab al Mandab (Red Sea), *Deep Sea Res., Part I*, *49*, 1551–1569, doi:10.1016/S0967-0637(02)00043-2.
- Siddall, M., E. J. Rohling, A. Almogi-Labin, C. Hemleben, D. Meischner, I. Schmeltzer, and D. A. Smeed (2003), Sea-level fluctuations during the last glacial cycle, *Nature*, *423*, 853–858, doi:10.1038/nature01690.
- Siddall, M., D. A. Smeed, C. Hemleben, E. J. Rohling, I. Schmeltzer, and W. R. Peltier (2004), Understanding the Red Sea response to sea level, *Earth Planet. Sci. Lett.*, *225*, 421–434, doi:10.1016/j.epsl.2004.06.008.
- Siddall, M., T. F. Stocker, R. Spahni, T. Blunier, J. McManus, and E. Bard (2006a), Using a maximum simplicity paleoclimate model to simulate millennial variability during the last four glacial cycles, *Quat. Sci. Rev.*, *25*, 3185–3197, doi:10.1016/j.quascirev.2005.12.014.
- Siddall, M., E. Bard, E. J. Rohling, and C. Hemleben (2006b), Sea-level reversal during T II, *Geology*, *34*(10), 817–820, doi:10.1130/G22705.1.
- Siddall, M., J. Chappell, and E.-K. Potter (2006c), Eustatic sea level during past interglacials, in *The Climate of Past Interglacials*, edited by F. Sirocko et al., pp. 75–92, Elsevier, Amsterdam.
- Siddall, M., T. F. Stocker, T. Blunier, R. Spahni, J. Schwander, J.-M. Barnola, and J. Chappellaz (2007), Marine Isotope Stage (MIS) 8 millennial variability stratigraphically identical to MIS 3, *Paleoceanography*, *22*, PA1208, doi:10.1029/2006PA001345.
- Sirocko, F. (2003), Global change: Ups and downs in the Red Sea, *Nature*, *423*, 813–814, doi:10.1038/423813a.
- Skinner, L. C., and H. Elderfield (2007), Rapid fluctuation in the deep North Atlantic heat budget during the last glaciation, *Paleoceanography*, *22*, PA1205, doi:10.1029/2006PA001338.
- Skinner, L. C., and N. J. Shackleton (2005), An Atlantic lead over Pacific deep-water change across Termination I: Implications for the application of the marine isotope stage stratigraphy, *Quat. Sci. Rev.*, *24*, 571–580, doi:10.1016/j.quascirev.2004.11.008.
- Skinner, L. C., H. Elderfield, and M. Hall (2007), Phasing of millennial climate events and Northeast Atlantic deep-water temperature change since 50 ka BP, in *Ocean Circulation: Mechanisms and Impacts—Past and Future Changes of Meridional Overturning*, *Geophys. Monogr. Ser.*, vol. 173, edited by S. Schmittner, J. C. H. Chang, and S. R. Hemming, pp. 197–208, AGU, Washington, D. C.
- Stanford, J. D., E. J. Rohling, S. E. Hunter, A. P. Roberts, S. O. Rasmussen, E. Bard, J. McManus, and R. G. Fairbanks (2006), Timing of meltwater pulse 1a and climate responses to meltwater injections, *Paleoceanography*, *21*, PA4103, doi:10.1029/2006PA001340.
- Stirling, C. H., T. M. Esat, K. Lambeck, and M. T. McCulloch (1998), Timing and duration of the Last Interglacial: Evidence for a restricted interval of widespread coral reef growth, *Earth Planet. Sci. Lett.*, *160*(3–4), 745–762, doi:10.1016/S0012-821X(98)00125-3.
- Stocker, T. F., and S. J. Johnsen (2003), A minimum thermodynamic model for the bipolar seesaw, *Paleoceanography*, *18*(4), 1087, doi:10.1029/2003PA000920.
- Stocker, T. F., D. G. Wright, and W. S. Broecker (1992), Influence of high-latitude surface forcing on the global thermohaline circulation, *Paleoceanography*, *7*, 529–541, doi:10.1029/92PA01695.
- Stuiver, M., and T. F. Braziunas (1993), Modeling atmospheric C-14 influences and C-14 ages of marine samples to 10,000 BC, *Radiocarbon*, *35*(1), 137–189.

- Stuiver, M., and P. M. Grootes (2000), GISP2 oxygen isotope ratios, *Quat. Res.*, *53*, 277–284, doi:10.1006/qres.2000.2127.
- Svensson, A., et al. (2006), The Greenland Ice Core Chronology 2005, 15–42 ka. Part 2: Comparison to other records, *Quat. Sci. Rev.*, *25*(23–24), 3258–3267, doi:10.1016/j.quascirev.2006.08.003.
- Thompson, W. G., and S. L. Goldstein (2005), Open-system coral ages reveal persistent suborbital sea-level cycles, *Science*, *308*(5720), 401–404, doi:10.1126/science.1104035.
- Thompson, W. G., and S. L. Goldstein (2006), A radiometric calibration of the SPECMAP timescale, *Quat. Sci. Rev.*, *25*(23–24), 3207–3215, doi:10.1016/j.quascirev.2006.02.007.
- Thunell, R. C., S. M. Locke, and D. F. Williams (1988), Glacio-eustatic sea-level control on Red Sea salinity, *Nature*, *334*(6183), 601–604, doi:10.1038/334601a0.
- Vinther, B. M., et al. (2006), A synchronized dating of three Greenland ice cores throughout the Holocene, *J. Geophys. Res.*, *111*, D13102, doi:10.1029/2005JD006921.
- Voelker, A. H. L. (2002), Global distribution of centennial-scale records for marine isotope stage (MIS) 3: A database, *Quat. Sci. Rev.*, *21*(10), 1185–1212, doi:10.1016/S0277-3791(01)00139-1.
- Wadley, M. R., G. R. Bigg, E. J. Rohling, and A. J. Payne (2002), On modelling present-day and last glacial maximum oceanic  $\delta^{18}\text{O}$  distribution, *Global Planet. Change*, *32*(2–3), 89–109, doi:10.1016/S0921-8181(01)00084-4.
- Waelbroeck, C., L. Labeyrie, E. Michel, J. C. Duplessy, J. F. McManus, K. Lambeck, E. Balbon, and M. Labracherie (2002), Sea-level and deep water temperature changes derived from benthonic foraminifera isotopic records, *Quat. Sci. Rev.*, *21*, 295–305, doi:10.1016/S0277-3791(01)00101-9.
- Waelbroeck, C., C. Levi, J. C. Duplessy, L. Labeyrie, E. Michel, E. Cortijo, F. Bassinot, and F. Guichard (2006), Distant origin of circulation changes in the Indian Ocean during the last deglaciation, *Earth Planet. Sci. Lett.*, *243*(1–2), 244–251, doi:10.1016/j.epsl.2005.12.031.
- Wang, Y. J., H. Cheng, R. L. Edwards, Z. S. An, J. Y. Wu, C. C. Shen, and J. A. Dorale (2001), A high-resolution absolute-dated Late Pleistocene monsoon record from Hulu Cave, China, *Science*, *294*(5550), 2345–2348, doi:10.1126/science.1064618.
- Werner, F., and K. Lange (1975), A bathymetric survey of the sill area between the Red Sea and the Gulf of Aden, *Geol. Jahrbuch D*, *13*, 125–130.
- Winter, A., A. Almogi-Labin, Y. Erez, E. Halicz, B. Luz, and Z. Reiss (1983), Salinity tolerance or marine organisms deduced from Red Sea Quaternary record, *Mar. Geol.*, *53*(1–2), M17–M22, doi:10.1016/0025-3227(83)90030-0.
- Wunsch, C. (2000), On sharp spectral lines in the climate record and the millennial peak, *Paleoceanography*, *15*(4), 417–424, doi:10.1029/1999PA000468.
- Yokoyama, Y., K. Lambeck, P. De Deckker, P. Johnston, and L. K. Fifield (2000), Timing of the Last Glacial Maximum from observed sea-level minima, *Nature*, *406*(6797), 713–716, doi:10.1038/35021035.
- Yokoyama, Y., T. M. Esat, and K. Lambeck (2001), Coupled climate and sea-level changes deduced from Huon Peninsula coral terraces of the last ice age, *Earth Planet. Sci. Lett.*, *193*(3–4), 579–587, doi:10.1016/S0012-821X(01)00515-5.
- 
- E. J. Rohling, National Oceanography Centre, Southampton, University of Southampton, Waterfront Campus, European Way, Southampton SO14 3ZH, UK.
- M. Siddall, Department of Earth Sciences, University of Bristol, Wills Memorial Building, Queen's Road, Bristol BS8 1RJ, UK. (siddall@ideo.columbia.edu)
- W. G. Thompson, Woods Hole Oceanographic Institution, 266 Woods Hole Road, Mail Stop 23, Woods Hole, MA 02543, USA.
- C. Waelbroeck, Laboratoire des Sciences du Climat et de l'Environnement, IPSL, CEA, CNRS, F-91198 Gif-sur-Yvette, France.